

Petra Vornanen

**OPTIMIZATION OF THE DIFFERENTIA-
TION EFFICIENCY FOR HUMAN PLU-
RIPOTENT STEM CELL-DERIVED COR-
NEAL ENDOTHELIAL CELLS**
with a focus on culture sub-
strates

Faculty of Medicine and Health
Technology
Master's thesis
January 2025

ABSTRACT

Petra Vornanen: Optimization of the differentiation efficiency for human pluripotent stem cell-derived corneal endothelial cells – with a focus on culture substrates

Master's thesis

Tampere University

Master's Programme in Biomedical Technology

Supervisors: Prof. Heli Skottman, PhD Kirsi Sepponen

Examiners: Prof. Vesa Hytönen, Prof. Heli Skottman

January 2025

Background and Aims:

Corneal blindness is the third leading cause of blindness globally, with corneal endothelium (CEn) dysfunction being the primary contributor. Currently, the only treatment is transplantation from cadaveric donors, but a significant shortage of donors poses a major challenge. A promising alternative is the use of human pluripotent stem cell (hPSC)-derived corneal endothelial cells (CEnCs). This study aimed to optimize the differentiation efficiency and purity of hPSC-derived CEnC-like cells by investigating the effects of different culture substrates. Additionally, the potential to shorten the differentiation protocol was evaluated.

Methods:

Human PSCs were differentiated into CEnC-like cells utilizing a previously established protocol with slight modifications: various culturing substrates and their combinations were tested, including laminin-332, laminin-411 and different concentrations of laminin 521, and the protocol duration was adjusted shorter. Both a human induced PSC (hiPSC) line and a human embryonic stem cell (hESC) line were used. To assess the effects of different substrates and shorter differentiation time, cell morphology was monitored throughout the process. To determine relative gene expression levels, RNA samples were collected on days 0 and 7 for real-time quantitative polymerase chain reaction (RT-qPCR) analysis using the $2^{-\Delta\Delta C_t}$ method. Additionally, cell culture samples were fixed for immunocytochemistry analyses on days 0 and 7.

Results and Conclusions:

None of the other substrates or their combinations remarkably affected differentiation efficiency, except for laminin-411, on which the cells failed to attach. Cell morphology remained consistent across all conditions. Gene and protein expression levels were also comparable between conditions. Concentration of laminin-521 did not affect the differentiation. The protocol was effective even in its shorter version, with cells differentiating and exhibiting morphology similar to those cultured under the standard protocol. These results suggest that the choice of culturing substrate does not substantially influence the purity of the cell population or negatively impact differentiation. However, further studies are required to optimize the differentiation process.

Keywords: cornea, corneal endothelium, corneal endothelial-like cell, extracellular matrix, pluripotent stem cell

The originality of this thesis has been checked using the Turnitin OriginalityCheck service.

The AI tools used in my thesis and the purpose of their use has been described below:

Tool name and version: OpenAI (2024). GPT-4: Large language model.
<https://chatgpt.com>

AI tool was used to check the grammar, fluency, consistency, and structure of the text.
All texts were initially written by the author.

I am aware that I am totally responsible for the entire content of the thesis, including the parts generated by AI, and accept the responsibility for any violations of the ethical standards of publications

PREFACE

This Master's thesis was conducted in Prof. Heli Skottman's Eye Regeneration research group at the Faculty of Medicine and Health Technology at Tampere University. I would like to express my heartfelt thanks to Prof. Heli Skottman for providing me the opportunity to carry out my thesis in the Eye Regeneration group and for her guidance throughout the writing process. Big thanks also to my other supervisor, PhD Kirsi Sepponen, for her support and guidance with the experimental work. I am equally grateful to the laboratory technicians, Hanna Pekkanen and Outi Melin, for their expertise and assistance in the laboratory. Finally, I would like to thank my family and friends for their invaluable support and encouragement during my university journey.

Tampere, 16 January 2025

Petra Vornanen

CONTENTS

1. INTRODUCTION	1
2. LITERATURE REVIEW.....	3
2.1 Structure and function of the cornea	3
2.2 Development of the cornea.....	6
2.3 Corneal blindness	8
2.4 Stem cells.....	11
2.4.1 Human embryonic stem cells (hESCs).....	11
2.4.2 Human induced pluripotent stem cells (hiPSCs)	12
2.5 Differentiation towards endothelial-like cells	13
2.6 The extracellular matrix (ECM)	16
2.6.1 ECM for culturing CEnCs	17
2.7 Differentiation efficiency and current problems	18
3. AIMS OF THE THESIS	22
4. MATERIALS AND METHODS	23
4.1 hPSC lines.....	23
4.2 Differentiation of hPSCs to CEnC-like cells.....	23
4.3 Characterization	25
4.3.1 Gene expression analysis	25
4.3.2 Immunocytochemistry	26
5. RESULTS	28
5.1 Matrix tests	28
5.2 Direct induction.....	37
5.3 LN521 concentration test.....	43
6. DISCUSSION.....	46
6.1 Matrix tests	46
6.2 Direct induction.....	50
6.3 LN521 concentration test.....	51
6.4 Study limitations	52
6.5 Future directions.....	52
7. CONCLUSIONS.....	54
REFERENCES.....	55
SUPPLEMENTAL METHODS.....	67

LIST OF SYMBOLS AND ABBREVIATIONS

AQP1	Aquaporin 1
AP2 α	Activating enhancer binding protein 2 α
BMP	Bone morphogenetic protein
CEn	Corneal endothelium
CEnCs	Corneal endothelial cells
c-Myc	cellular Myelocytomatosis oncogene
DKK2	Dkkopf-related protein 2
DM	Descemet's membrane
DMEK	Descemet membrane endothelial keratoplasty
DSAEK	Descemet stripping endothelial keratoplasty
E8	Essential 8 TM medium
EB	Embryoid body
ECM	Extracellular matrix
ECD	Endothelial cell density
EMT	Epithelial-mesenchymal transition
ESC	Embryonic stem cell
FECD	Fuchs' endothelial corneal dystrophy
FOXC1	Forkhead box C1
hESC	Human embryonic stem cell
hiPSC	Human induced pluripotent stem cell
ICM	Inner cell mass
Klf4	Krüppel-like factor 4
LN	laminin
NCAD	N-cadherin
NCC	Neural crest cell
MET	Mesenchymal-endothelial transition
OCT4	Octamer-binding transcription factor 4
PAX6	Paired box 6
PITX2	Paired-like homeodomain transcription factor 2
PK	Penetrating keratoplasty
POM	Periocular mesenchyme
PSC	Pluripotent stem cell
RA	Retinoic acid
RPE	Retinal pigment epithelium
RT-qPCR	Real-time quantitative polymerase chain reaction
SLC4A4	Sodium bicarbonate cotransporter
Sox2	Sex Determining Region Y box 2
TE	Trophectoderm
TGF- β	Transforming growth factor β
ZO-1	Zona occludens 1

1. INTRODUCTION

Vision has a pivotal role in human interaction with others and the surrounding world. Proper eye function requires a healthy and transparent outermost layer, the cornea. The cornea not only protects the eye's internal structures but also contributes significantly to its refractive power. (Sridhar, 2018)

Corneal endothelium (CEn) is the innermost layer of the cornea, consisting of a monolayer of tightly packed hexagonal corneal endothelial cells (CEnCs). These cells are responsible for maintaining corneal transparency by transporting water out of the stroma. However, human CEnCs lack the ability to divide *in vivo*, resulting in no regenerative capacity through cell division. Damage to the CEn can compromise its barrier function, leading to corneal edema, opacity, and ultimately impaired vision. (Català et al., 2022)

Corneal blindness is the third most typical cause of blindness globally, following cataract and glaucoma, with 10 million people suffering bilateral corneal blindness. In developed countries, the primary cause of corneal blindness is CEn dysfunction, with corneal transplantation being the only available treatment. However, in 2012, approximately 12.7 million people were waiting for a corneal transplant, meaning that only 1 in 70 patients in need could receive the procedure. (Alonso-Alonso et al., 2023; Gain et al., 2016) This highlights a significant shortage of donor corneas and underscores the need for alternative treatment approaches.

One promising option is the use of human pluripotent stem cell (hPSC) based applications, where CEnC-like cells are derived either from embryonic stem cells (ESCs) or induced pluripotent stem cells (iPSCs). This approach eliminates the reliance on donor corneas and hiPSC reduces also the risk of rejection. However, protocols for differentiating CEnCs from hPSCs are still in the early stages of development, with one major challenge being the ability to obtain a pure population of differentiated cells. (Català et al., 2022) Additionally, these protocols are highly time-consuming and complex, requiring still a lot of optimizations.

The aim of this thesis was to enhance the differentiation of hPSCs into CEnC-like cells and to shorten the differentiation protocol while maintaining its efficiency. The thesis begins with a literature review covering the CEn, its roles, and functions, followed by a discussion of its development, injuries, and the current state of hPSC-CEnC differentiation protocols. The experimental section describes the differentiation and characterization of CEnC-like cells with different substrates, followed by the presentation and discussion of results and a conclusion summarizing the findings.

2. LITERATURE REVIEW

2.1 Structure and function of the cornea

A normal human eye has a circumference of approximately 69 to 85 mm. It is composed of three main layers which can be further categorized into more detailed structures. The outermost layer of the eye acts as a support and consists of cornea, opaque sclera, and limbus. The middle uveal part of the eye includes the central vascular layer of the globe, ciliary body, and choroid. The innermost eye layer is the retina which can be further divided into ten retinal layers. (Kels et al., 2015)

The cornea is a transparent, non-vascular tissue that, along with sclera, forms the outer covering of the eye. The main functions of the cornea are protecting the structures inside the eye by acting as a structural barrier, impacting the refractive power of the eye, and focusing light rays on the retina. (Sridhar, 2018) Even though the cornea is an avascular tissue, it is highly dependent on the components of the blood to stay healthy. These components are carried by small vessels in the edges of the cornea as well as via the aqueous humor and tear film. The cornea is also heavily innervated and sensitive tissue. (DelMonte & Kim, 2011)

The cornea is convex and aspheric tissue. It has an oval shape horizontally and the diameter varies between 11.04 and 12.50 mm in males and 10.7 and 12.58 mm in females. The anterior curvature of the cornea measures 7.8 mm and the posterior is approximately 6.5 mm. The thickness is 551-565 μm in the central cornea and 612-640 μm in the peripheral cornea. This variation is due to the increasing volume of collagen in the peripheral stroma. Cornea has a refractive index of 1.376 and it constitutes approximately 70% of total refraction. (Sridhar, 2018)

The human cornea contains 5 layers of which 3 are cellular and 2 acellular. The cellular layers are epithelium, stroma, and endothelium and the acellular interfaces are Bowman's membrane and Descemet membrane (DM) (Figure 1.). The epithelium forms the outermost layer of the cornea acting as the first barrier to the outside environment. It is an essential part of the tear film-cornea boundary that is crucial for the eye's refractive ability. (DelMonte & Kim, 2011) The epithelium is around 50 μm thick and consists of 5 - 7 layers of nonkeratinized stratified squamous epithelium. Developmentally it originates from surface ectoderm between 5 and 6 gestational weeks. The corneal epithelium has

three cell types: superficial cells, wing cells, and basal cells. In addition to limbal stem cells and transient amplifying cells, the only corneal epithelial cells that can undergo mitosis are basal cells. Therefore, basal cells serve as the source of wing and superficial cells. (Sridhar, 2018)

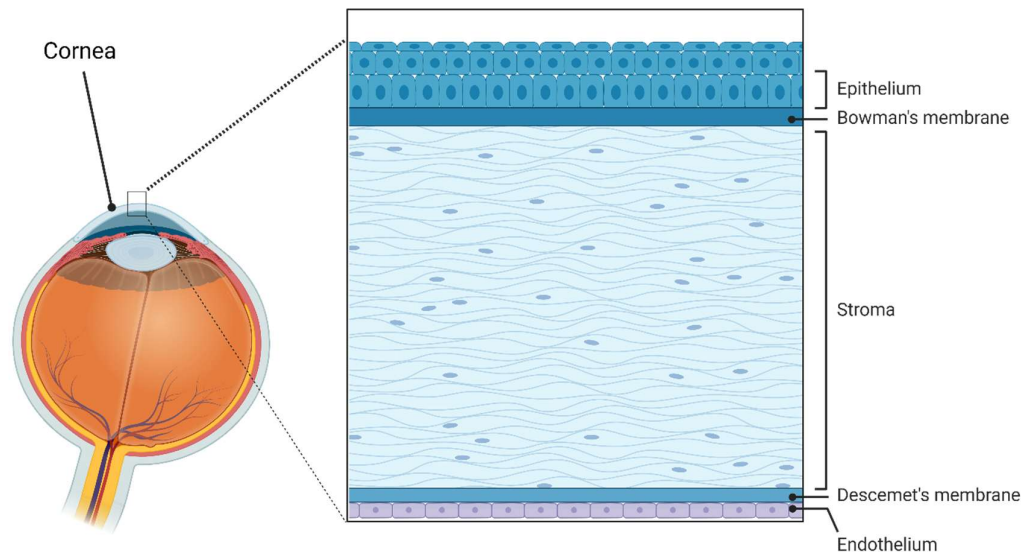


Figure 1. *Illustration of the five layers of the human cornea. Created with Biorender.com*

Bowman's layer is an 8 to 12 μm thick membrane that lies between epithelium and stroma. It is acellular and consists of irregularly positioned collagen fibrils, mainly collagen type I. (Wilson, 2020) Also, proteoglycans can be found in its structure. Bowman's layer supports the cornea in maintaining its shape. It does not regenerate, so in the event of an injury, a scar may form. (Sridhar, 2018) The layer develops between 13 and 19 weeks of gestation, with keratocytes present during early corneal development. However, if keratocytes are retained in the membrane, they cause a distinct thickening of Bowman's layer. (Wilson, 2020)

Beneath the Bowman's layer is the corneal stroma proper which constitutes about 90% of the corneal thickness. The mechanical properties of the stroma are required for strength and shape maintenance of the cornea. The stroma comprises extracellular matrix (ECM) molecules, water, and keratocytes that synthesize the stromal ECM. Keratocytes are neural crest-derived cells that are vital for the development of the stroma as well as for its maintenance. The primary component of the stromal ECM is collagen I

which is organized into fibrils and higher ordered structures. (España & Birk, 2020) Besides collagen I, there are also four leucine-rich proteoglycans, namely decorin, lumican, keratocan, and mimecan. In addition to these, there are also biglycan and fibromodulin. (Meek & Knupp, 2015)

DM is the basement membrane for the corneal endothelium (CEn) and its development begins at the 8th gestational week (de Oliveira & Wilson, 2020; Sridhar, 2018). DM separates the posterior corneal stroma from the CEn. It is a thick, dense and relatively transparent cell-free matrix containing collagenous and non-collagenous components. The four main components are laminins, collagen type IV, nidogens, and perlecan. DM includes several common components found in other basement membranes, but despite this, it has a unique composition compared to basement membranes of other organs. The role of DM is not just to act as a binding site for corneal endothelial cells (CEnCs), but also to contribute to corneal homeostasis and clarity, as well as take part in the modulation of corneal hydration. Together with CEn, the barrier functions of DM bidirectionally adjust the passage of macromolecules, such as growth factors and nutrients, between the aqueous humor and the corneal stroma. This function is essential for metabolism of keratocytes, nerves, and epithelium. Macromolecule passage is facilitated by the open, porous structure of DM, maintained by the hexagonal lattice organization of collagen type VIII. The barrier functions of DM are crucial in avoiding the formation of myofibroblasts and stromal fibrosis. In this way, the function of DM prevents corneal opacity caused by growth factors that are normally abundant only in the aqueous humor. Pathophysiological modulations of DM are involved also in many corneal diseases such as Fuchs' endothelial corneal dystrophy (FECD). (de Oliveira & Wilson, 2020) The role of laminins and other ECM components is discussed in greater detail in the upcoming chapter.

The CEn is a cell monolayer on the posterior surface of the cornea, on top of DM. It keeps the cornea transparent by transporting water out of the stroma. CEn is composed of terminally differentiated CEnCs that are flat and highly polarized. They have hexagonal apical surfaces from which they are in touch with aqueous humor of the anterior chamber and irregular basal surfaces that are in contact with DM. These cells have different types of enzymatic pumps which create ionic gradients and thereby extract water out of the stroma. (He et al., 2016) One such pump is the sodium-potassium pump (Na^+/K^+ ATPase). In addition to its pumping function, passive diffusion also plays a role in maintaining transparency and is regulated by the tight junction protein zonula occludens-1 (ZO-1). (Bogerd et al., 2019)

As mentioned above, CEnCs are terminally differentiated meaning that their mitotic regeneration in humans is very limited (Qazi et al., 2010). They are halted in the G1 phase of the cell cycle, influenced by three mechanisms: cell-cell contact-dependent inhibition, absence of efficient growth factor stimulation, and reduction of S-phase by transforming growth factor beta 2 (TGF- β 2). For this reason, CEnCs react to minor damage by stretching centripetally into the injured area. (Zavala et al., 2013) A high CEnC density is needed to maintain the pumping capacity and functionality of the CEn. When the cell density falls under a critical threshold of around 400-700 cells/mm², the normal functions of the CEn are impaired. (Roy et al., 2015) The mechanisms for CEnCs to repair damage are discussed in more detail below.

2.2 Development of the cornea

To utilize the hPSC-based applications, it is important to understand the development of the human cornea and the factors affecting it. The development of the cornea begins around gestational day 33 when the lens cup detaches from the surface ectoderm (Van Cruchten et al., 2017). It is a multi-step process that includes cellular interactions between multiple ectodermal-derived tissues. The corneal epithelium forms from interactions between the cranial ectoderm and the neural ectoderm-derived optic vesicles, while the CEnCs and stromal keratocytes form from periocular mesenchyme (POM), more specifically from migrating neural crest cells (NCCs). To form the CEn, the NCCs go through mesenchyme-to-endothelial transition (MET) and form a cell layer on the posterior surface of the cornea. (Hatou & Shimmura, 2019; Lwigale, 2015) This occurs around 47-48 days of gestation (Graw, 2003). The corneal stroma is the last layer to arise during corneal development and it results from the second wave of NCC migration (Lwigale, 2015). Finally, the CEnCs produce a basement membrane, DM, to separate the endothelium from the stroma (Hatou & Shimmura, 2019).

The mechanisms underlying the migration of NCCs and maturation of the CEn are not fully understood. The migration of NCCs initiates with epithelial-mesenchymal transition (EMT) and the cells move to the periocular region and subsequently arrive at the area beneath the CEn. Important contributors in this process are TGF- β , bone morphogenetic protein (BMP), and Wnt signaling. (Hatou & Shimmura, 2019) Overall, the TGF- β superfamily of growth factors, which include BMPs, are widely known for their capacity to trigger EMT during development. Besides this, they have also various other roles during development, such as in axis formation, germ-layer specification, and organogenesis. In

fully developed organisms, the TGF- β superfamily is needed for tissue homeostasis. One of the many downstream pathways of TGF- β superfamily is the Smad pathway. The Smads are intracellular signaling molecules that after stimulation accumulate to nucleus and modulate transcription. In variety of endothelial, epithelial, fibroblast, and tumor cells TGF- β activates for example Smad2/3 and Smad1/5/8 complexes. (Wu & Hill, 2009) Wnt signaling pathway consists of secreted growth factors that are important for stem cell renewal, cell proliferation and cell differentiation during development as well as during adult tissue homeostasis. The best known Wnt signaling pathway is the Wnt- β -catenin pathway of which function is based on the degradation of β -catenin in the absence of Wnt proteins. The process is mediated by a destruction complex, which is composed of scaffolding proteins and kinases. If Wnt proteins are present, β -catenin is stabilized, and it can act as transcriptional co-activator. One of the destruction complex kinases, GSK3, can be a target for inhibition and thereby the Wnt pathway can be artificially activated. (Steinhart & Angers, 2018)

During the maturation of the CEn, MET may occur in reverse, driven by various transcription factors, including Forkhead box C1 (FOXC1), paired box 6 (PAX6), and paired-like homeodomain transcription factor 2 (PITX2), among others. However, it is not clear whether they work during the migration or the maturing process. (Hatou & Shimmura, 2019) Though, it is known that the development of the anterior segment of the eye, which includes the cornea, relies on the proper activity of two of those factors: FOXC1 and PITX2 (Ittner et al., 2005). TGF β 1 and TGF β 2 are observed to enhance the levels of FOXC1 and PITX2 expression and in the CEn, they adjust cell proliferation, cell morphology, and collagen expression. PAX6 is a master gene in eye development, and it is needed for the development of all layers of the cornea. PAX6 expression is regulated by various molecules, such as TGF β 1, TGF β 2, and BMP7. (Zavala et al., 2013) Also, retinoic acid (RA), a significant regulator of embryonic development and an important morphogen signalling molecule, plays a role in corneal development. RA is involved in controlling the NCC induction, migration, survival, and differentiation. In mice and zebrafish, RA enhances the expression of PITX2 in the POM, and this elevated PITX2 expression further regulates the migration and differentiation of ocular NCCs via multiple downstream pathways, such as Wnt- β -catenin signalling pathways. (Williams & Bohnsack, 2019) This suggests a role for RA in the development of CEnCs as well.

2.3 Corneal blindness

Being the outermost layer of the eye, the cornea is in direct contact with the environment and is therefore susceptible to possible injuries due to burns, abrasions, contact lens problems, insufficient tear production, infections, and other disease conditions, along with refractive surgeries (Saghizadeh et al., 2017). Thus, corneal wound healing is not only of interest to basic science but also represents an important medical concern that requires proper management (Ljubimov & Saghizadeh, 2015). The response to injury differs between the three primary cell types of the cornea, though they also have some similarities. The similarities involve cell migration and proliferation, the involvement of growth factors and cytokines, as well as the restructuring of the ECM. The differences are related to the distinct behaviour of the healing cells. The regeneration of the epithelial layer is dependent on limbal stem cells that proliferate and migrate from the peripheral limbal area to the centre of the cornea and there renew the epithelial layers. (Saghizadeh et al., 2017) Corneal stromal wound healing includes changes in ECM caused by the death of keratocytes, secretion of proinflammatory and profibrotic cytokines, the temporary presence of cells that are not typically part of the stroma (e.g. macrophages), and the release of ECM-deteriorating enzymes by activated cells. (Ljubimov & Saghizadeh, 2015) Next, I will focus on the matters related to degeneration of CEn.

The amount of healthy CEnCs decreases with age, being 6000 cells/mm² in newborns and around 3500 cells/mm² in young adults. The degeneration continues at about 0,6% per year. (Gupta et al., 2021) Thus, age is a risk factor for causing corneal blindness. However, the number of CEnCs can diminish dramatically following CEn damage due to some trauma (Mimura et al., 2013), making corneal blindness a problem for children and young adults as well. The cause of the trauma can be, for example, infection, iatrogenic damage after surgery, or genetic disease such as FECD which is discussed in more detail below. The damage disrupts the CEn's barrier functions, resulting in corneal swelling and opacity. These impair vision and lead eventually to blindness. (Català et al., 2022) As mentioned earlier, human CEnCs are halted in the G1 phase of the cell cycle and are therefore incapable of dividing and repairing themselves *in vivo*. The cell cycle arrest is due to cell-cell contact-dependent inhibition, absence of effective growth factor stimulation, and suppression of S-phase by TGF- β 2. (Zavala et al., 2013) Dead or damaged CEnCs are replaced by their neighbouring cells via migration and cell enlargement with reported TGF- β -driven EMT (Saghizadeh et al., 2017). Although this restores the barrier functions of the CEn, the decreased cell density will at last cause the pumping capacity to decrease. Besides this, the CEnCs lose their hexagonal morphology. The

critical endothelial cell density (ECD) is 500 cells/mm² and when ECD drops below this threshold, CEnC decompensation takes place. This results in the corneal edema discussed above. (Van den Bogerd et al., 2018) Cell density is also a crucial thing when defining the quality of donor corneas. For a transplantation to be successful, cell densities typically need to exceed 2500 cells/mm². (Moshirfar et al., 2021) Around one-third of donor corneas are rejected because of inadequate CEn quality or the presence of infections (Alonso-Alonso et al., 2023).

FECD is an example of a disease that causes CEnC damage. It is a slowly progressive hereditary disease characterized by the degeneration of CEnCs and the development of guttate which are outgrowth of DM. FECD advances gradually to CEnC decline, the resultant loss of corneal dehydration, and corneal edema of the stroma or epithelial layers, thereby leading to eye pain, glare, halos, and reduced visual acuity. (Moshirfar et al., 2024) FECD is caused by a complicated blend of environmental and genetic factors. It can be classified as early-onset or late-onset (Feizi, 2018). The early-onset version of FECD leads to corneal deterioration at an early age due to a notably thickened DM. The thickness of the DM can reach up to 38 µm, compared to 5-10 µm in normal corneas. In the late-onset version, the thickness of the DM also increases, thus distinctly from early-onset: the overall thickness of DM grows, but the anterior layers remain comparatively intact. (Eghrari & Gottsch, 2010) Following changes in the CEn and DM, stromal edema also occurs, followed by alterations in the epithelium, such as cell loss and abnormal ECM production (J. Zhang et al., 2019). FECD is typically treated with surgery, with standard procedures including endothelial keratoplasty techniques, such as Descemet membrane endothelial keratoplasties (DMEK) and Descemet's stripping automated endothelial keratoplasty (DSAEK) (Röck et al., 2017) which are further discussed below.

In developed countries, the leading cause of corneal blindness is CEnC dysfunction. Currently, the only treatment option for CEnC failure is human donor tissue-dependent surgical transplantation and it is the most common reason for corneal transplantation globally. (Alonso-Alonso et al., 2023) In recent years, the advancements in corneal transplantation techniques have transformed the field of corneal transplant surgery. In the case of CEnC damage, the endothelial keratoplasty has replaced the penetrating keratoplasty (PK), meaning transplanting the full thickness cornea. The most used ways to only repair the CEn damage are DMEK and DSAEK, the first one mentioned being the golden standard. (Röck et al., 2017) In DMEK, the CEn layer is transplanted with only DM as its carrier when in DSAEK also part of the stromal interface is transplanted (Trinidad & Eliazar, 2019). These methods have many advantages over PK, for example,

minimal invasiveness, lower rate of rejection, minimal refractive shift and particularly rapid visual improvement (Röck et al., 2017).

However, the amount of transplantable-grade donor CEn is restricted and there is a worldwide shortage of corneal transplant tissue. In 2012 approximately 185 000 people from 116 different countries received a corneal transplant but at the same time, 12,7 million people were still waiting for the transplantation. This means that there was only one cornea accessible for every 70 patients in need. (Ali et al., 2021; Gain et al., 2016) Methods to regenerate the CEn provide a solution to the tissue shortage and new treatment options. The regeneration could happen through the primary culture of CEnCs or the *de novo* generation from hPSCs. However, there are many challenges to overcome. The biggest challenge for primary cultures is to force the quiescent cells to proliferate without EMT which would eventually cause a cellular loss of function. Also, donor-related factors, such as cause of death, age, and use of drugs, could affect the cell behavior and the success of the *in vitro* culture. (Català et al., 2022) Kinoshita et al. conducted the first clinical trials involving the injection of cultured primary human CEnCs derived from donor corneas into the anterior chamber of a patients having bullous keratopathy with no detectable CEnCs. To ensure the cell adhesion to the correct location in the CEn, patients were positioned face-down for three hours. This approach successfully restored the corneal transparency and obtained a cell density of more than 500 cells/mm². (Kinoshita et al., 2018) This trial was a significant breakthrough in treatment strategies for CEnC dysfunctions. However, to successfully establish primary CEnC cultures, the donor must be under 30 years old, as younger cells exhibit better proliferation and greater sensitivity to growth factors (Choi et al., 2014).

The differentiation of hPSCs to CEnCs provides several benefits, such as more rapid *in vitro* expansion and avoidance of the need for donor corneas. Thus, the application of hPSC is not free from challenges either. The biggest one is cell purity since undesired cell populations often arise during differentiation. Also, the safeness and functionality of these cells must be demonstrated. (Català et al., 2022) Hirayama et al. conducted the first-in-human clinical study using hiPSC-derived CEnCs. A patient with bullous keratopathy was treated via injection of these cells. The outcomes were promising, with partial enhancement in corneal swelling, transparency, and visual acuity observed, and no clinical adverse events reported. However, pigmentation of the transplanted cells and *de novo* gene mutation were noted despite pre-clinical testing. By analyzing the surface markers of their hiPSC-derived CEnCs, they also identified the potential presence of precursor cells among the differentiated population. (Hirayama et al., 2025) This trial

highlights the remaining challenges associated with the clinical applications of hPSC-derived cells.

2.4 Stem cells

Stem cells are undifferentiated cells that are capable of self-renewing and differentiating into various other cell types and thereby producing diverse tissues. Stem cells can be found in both embryos and adult tissues. (Larijani et al., 2012) They have different stages of specialization, and their developmental potency depends on the stage they are in, either totipotent, pluripotent, multipotent, or unipotent. Totipotent stem cells have the greatest developmental potency since they can divide and differentiate into cells of the whole organism. An example of a totipotent cell is a zygote which can form any of the three germ layers as well as the extraembryonic structures. (Zakrzewski et al., 2019) In this literature review, I will focus on PSCs only.

Six days after fertilization, a blastocyst is formed. It consists of two different cell layers: inner cell mass (ICM) and trophectoderm (TE). PSCs are in the ICM, and these cells can give rise to all three germ layers (mesoderm, endoderm, and ectoderm) but not the extraembryonic structures, such as placenta. PSCs of the human blastocyst are called human embryonic stem cells (hESCs). hESCs as well as human induced pluripotent stem cells (hiPSCs) are examples of this stage of specialization. (Zakrzewski et al., 2019) Both cell types are widely used in research because of their capability to differentiate into various cell types, and their relevance in disease modeling, regenerative medicine, and drug discovery (Pera et al., 2000; Singh et al., 2015). hESCs and hiPSCs are discussed in more detail below.

2.4.1 Human embryonic stem cells (hESCs)

Human ESCs are PSCs obtained from the ICM of a blastocyst stage embryo 5 to 8 days after fertilization. (Lewis et al., 2020) In 1998 human ESCs were first time successfully isolated from a donated embryo and grown in a laboratory (Thomson et al., 1998). Since then, the isolation and culture of new hESC lines under diverse methods and culture conditions have been reported in multiple studies. Usually, hESCs are derived from poor-quality preimplantation embryos donated for research. (Skottman, 2010) In general, hESCs are cultured in a manner similar to other mammalian cells, but three key factors essential for maintaining pluripotency must be carefully selected: the culture medium, substrate, and passage method. Initially, the hESCs colonies were cultured on top of

mouse embryonic fibroblasts with media containing serum. However, the reliance on the use of feeder cells and serum was problematic because of their nonhuman origin and high batch-to-batch variation. This led to the development of more defined, animal-free substances for culturing, such as recombinantly produced laminins as substrates. (Lewis et al., 2020)

Human ESCs offer a powerful tool for studying early human embryology, developing cell replacement therapies to treat different diseases, and investigating disease mechanisms *in vitro*. However, their use raises significant ethical concerns, as harvesting these cells requires the destruction of a human embryo. (Colman & Dreesen, 2009; Volarevic et al., 2018) Due to these ethical issues, the interest towards alternative PSC sources, such as hiPSCs, has increased.

2.4.2 Human induced pluripotent stem cells (hiPSCs)

Human iPSCs are embryonic-like PSCs derived from somatic cells by direct reprogramming. This method was established by Takahashi and Yamanaka in 2006 when they first showed that iPSCs can be generated from mouse somatic cells by retrovirus-mediated transfection of four transcription factors. In 2007, they reprogrammed adult human somatic cells to generate hiPSCs. The four needed factors are Octamer-binding transcription factor 4 (Oct4), Sex Determining Region Y box 2 (Sox2), cellular Myelocytomatosis oncogene (c-Myc), and Krüppel-like factor 4 (Klf4). (Takahashi et al., 2007) Oct4 is required to induce and maintain cellular pluripotency and it is found in all PSCs during embryogenesis and from undifferentiated ESCs. Sox2 interacts with Oct4 to modulate the expression of genes participating in maintaining pluripotency. It is crucial for the development of organs and tissues, and it is expressed also in the later phases of development, particularly in neural stem cells. Similarly to Sox2, also Klf4 interacts with Oct4, and it is required, for example, to activate transcription factor Nanog. Besides the activation of specific genes, epigenetic changes, in which c-Myc plays a role, are also necessary to inhibit cell differentiation or induce dedifferentiation. (Aguirre et al., 2023)

The hiPSCs technology offers a way to circumvent the ethical issues related to hESCs, enabling the use of stem cells in cell therapies and research without requiring the destruction of embryos. It is shown that the *in vivo* and *in vitro* features of hiPSCs are similar to those of hESCs, including the ability to self-renew and differentiate into various cell types. (Menon et al., 2016) Another advantage of hiPSCs is their potential for personalized medicine, as reprogrammed cells can be obtained from the patient. This removes

the risk of immune rejection after cell transplantation. However, the use of hiPSCs or hESCs is not entirely risk-free and safety concerns must also be addressed when considering the clinical application of hPSCs. The pluripotency of hPSCs is both an advantage and a challenge: while their exceptional capability to differentiate into hundreds of cell types is highly valuable, it also makes them challenging to control after *in vivo* transplantation. If undifferentiated hPSCs are transplanted, there is a risk for teratomas – tumours containing cells from all three germ layers. A safer option is to differentiate hPSCs into the desired and mature cell type before transplantation. Therefore, more efficient methods are needed to produce purified populations of differentiated cells derived from hiPSCs. (Volarevic et al., 2018)

2.5 Differentiation towards endothelial-like cells

Differentiation of PSCs into CEnC-like cells *in vitro* typically mimics the developmental processes outlined above: the first step is differentiation from PSCs to NCCs, followed by differentiation into CEnC-like cells (Hatou & Shimmura, 2019). Based on the current literature in the field, various methods have been established for the differentiation of CEnCs. Examples of differentiation protocols are summarized in Table 1. A common feature among these differentiation protocols is the modulation of TGF- β , Wnt, and BMP signalling pathways. One popular method for inducing NCCs from PSCs is dual-SMAD inhibition, which involves the simultaneous inhibition of TGF- β -SMAD-2/3 and BMP-SMAD-1/5/8 signaling pathways. (Ng et al., 2023) In many protocols, TGF- β signalling is blocked using SB431542 (Chen et al., 2021; Grönroos et al., 2021; McCabe et al., 2015; Wagoner et al., 2018; Zhao & Afshari, 2016). However, these protocols differ in the additional substances used alongside SB431542 to achieve dual-SMAD inhibition (see Table 1). For example, McCabe et al. used BMP inhibitor Noggin, while Chen et al. utilized dorsomorphin homolog 1 (DMH1) to block BMP signaling.

Interestingly there is also alternative approaches, as Li et al. did not utilize dual-SMAD inhibition in their protocol. Instead, they used basic fibroblast growth factor (bFGF) and RA to induce NCCs (Li et al., 2022). As discussed previously, RA is involved in controlling NCC induction and acts as an important morphogen signalling molecule during embryonic development (Williams & Bohnsack, 2019). Therefore, its use in inducing NCCs is a logical choice. Similarly, Grönroos et al. incorporated RA in their protocol, using it throughout the differentiation process with varying concentrations. As an additional example of different approaches, Zhang et al. used a completely different method since

they utilized the formation of embryoid bodies (EB) and then co-cultured them with corneal stromal cells (K. Zhang et al., 2014).

Once the PSCs have been induced into NCCs, the next step is to produce CEnC-like cells. There is not a universal way to do it, hence SB431542 is often used in this step as well (see Table 1). It is known that SB431542 preserves the normal endothelial phenotypes of cultured CEnCs (Hachana & Larrivé, 2022) so it is justified to use also in the later stages of differentiation protocols. As seen from Table 1, there are various other substances also used to induce CEnC differentiation. For instance, Dickkopf-related protein 2 (DKK2) is a Wnt signaling inhibitor (Wagoner et al., 2018) which again leads us back to the fact that TGF- β , Wnt, and BMP signalling pathways are capitalized in these protocols. Despite the various methods used, all protocols successfully differentiated CEnC-like cells, that express CEnC markers, such as Na⁺/K⁺ ATPase, and have polygonal morphology.

Overall, the differentiation of CEnC-like cells relies on insights from developmental biology. However, as the complete developmental process of CEnCs is not yet fully understood, designing the optimal combination of growth factors and signaling molecules for differentiation remains a challenge. For clinical applications, it is crucial to avoid undefined components and animal-derived materials in these protocols. Additionally, the protocols are often lengthy and time-consuming (see Table 1), which poses a limitation when aiming for clinical implementation. While considerable progress has been made, substantial work remains ahead.

Table 1 provides a comprehensive overview of the various protocols used for CEnC differentiation. However, this thesis focuses specifically on the effects of culturing substrates, and the remainder of this literature review will emphasize that aspect. A key factor in differentiation protocols is the matrix on which the cells are cultured. The role of the matrix is explored in more detail in the next chapter.

Table 1. Examples of differentiation protocols for generating CEnC-like cells from hPSCs.

Protocol	Differentiation Method	Medium	Matrix	Result
Li et al. 2022	Two step method: to NCCs with bFGF and RA, to CEnCs with Y27632 and SB431542	Neural crest differentiation medium, corneal endothelial differentiation medium	Matrigel	Within 22 days, cells expressed CEnC markers (e.g. ZO-1, Na ⁺ /K ⁺ ATPase, AQP1) and had hexagonal morphology
Grönroos et al. 2021	Differentiation with SB431542, CHIR99021, and varying concentration of RA	E8 Flex medium, serum-free basal medium with supplements	LN521	After one week, cells expressed CEnC markers (e.g. ZO-1, Na ⁺ /K ⁺ ATPase, CD166) and had hexagonal morphology
Chen et al. 2021	Three-step method: to NCCs with SB431542, DMH1, to CEnCs with A769662, AT13148, maturation with EGF and CHIR99021	Basal medium with supplements, chemical defined medium (CDM)	Matrigel	After 22 days, cells expressed CEnC markers (e.g. ZO-1, Na ⁺ /K ⁺ ATPase, AQP1) and had hexagonal morphology
Wagoner et al. 2018	Two-step method: to NCCs with SB431542 and CHIR99021, to CEnCs with B27, PDGF-BB and DKK-2	E8 Flex medium, basal medium with supplements	LN521	After minimum of 25 days, cells expressed CEnC markers (e.g. ZO-1, Na ⁺ /K ⁺ ATPase, AQP1) and had hexagonal morphology
Zhao and Afshari, 2016	Three-step method: to eye field stem cells with SB431542, LDN193189 and IWP2, to NCCs with CHIR9902, to CEnCs with SB431542 and H-1125	Serum-free basal medium with supplements, HE-SFM with supplements	Matrigel for EFSCs and NCCs, FNC Coating Mix for CEnC induction	After 21 days, cells expressed CEnC markers (e.g. Na ⁺ /K ⁺ ATPase, N-Cadherin) and had hexagonal morphology
McCabe et al. 2015	Two-step method: to NCCs with SB431542 and Noggin, to CEnCs with PDGF-BB, DKK-2 and FGF2	Serum-free basal medium with supplements	Matrigel	After 3-4 weeks, cells expressed CEnC markers (e.g. ZO-1, Na ⁺ /K ⁺ ATPase) and had hexagonal morphology
Zhang et al. 2014	First EB formation, then EBs co-cultured with corneal stroma cells with presence of B27, EGF and bFGF	Basal medium with supplements, lens epithelial cell-conditioned medium	Low adherence culture dish for EBs, fibronectin, laminin and heparin sulfate for co-culture	After 3 weeks, cells expressed CEnC markers (e.g. ZO-1, Na ⁺ /K ⁺ ATPase) and had hexagonal morphology

Abbreviations: NCC: neural crest cell, bFGF: basic fibroblast growth factor, RA: retinoic acid, CEnC: Corneal endothelial cell, Y27632: ROCK inhibitor, SB431542: activin/ BMP/ TGF-beta pathway inhibitor, CHIR99021: GSK-3 inhibitor and Wnt pathway activator, DMH1: dorsomorphin homolog 1, A769662: activator of AMP-activated protein kinase, AT13148: ATP-competitive inhibitor of multiple AGC kinases, EGF: epidermal growth factor, PDGF-BB: platelet-derived growth factor BB, DKK-2: Dickkopf-related protein 2, LDN193189: inhibitor of BMP type I receptors, IWP2: Wnt pathway inhibitor, H-1125: ROCK inhibitor, FGF2: Fibroblast growth factor 2, EB: Embryoid body, HE-SFM: Human endothelial serum-free media, LN521: Laminin-521, ZO-1: Zona Occludens 1, AQP1: Aquaporin 1

2.6 The extracellular matrix (ECM)

The ECM is a non-cellular part of all tissues and organs, and it offers physical support for the cellular constituents as well as biochemical and biomechanical cues that are required for morphogenesis, differentiation and homeostasis of tissues. Overall, the ECM is composed of water, fibrous proteins and proteoglycans, but each tissue has an exclusive composition of ECM suitable for the needs of that specific tissue. The main fibrous proteins found in ECM are collagens, fibronectins, elastins, and laminins. Proteoglycans are built of glycosaminoglycan chains that are covalently attached to a core protein. Cells adhere to their ECM via receptors, such as integrins. Through this, cells cytoskeleton is linked to the ECM, and this enables migration through the matrix. The ECM itself is not stable, as it is continuously being reorganized. (Frantz et al., 2010) However, ECM components are precisely organized and even minor modifications, such as a change of one amino acid in one ECM component, can cause alterations in cell-matrix interactions and in cellular phenotype and thereby change the physicochemical properties of the whole tissue (Järveläinen et al., 2009).

As mentioned earlier, during corneal development, human CEnCs produce their DM to separate the CEn from the stroma (Hatou & Shimmura, 2019). During prenatal development, CEnCs produce an anterior thin lamella layer which remains unchanged throughout life. However, CEnCs continue producing ECM components even after prenatal development *in vivo*. While the secretion of collagen type VIII decreases, the secretion of collagen type IV remains consistent. The DM thickens on the posterior side over time and becomes more non-lamellar and homogenous compared to its prenatal structure. If the function of CEnCs is somehow disrupted, the formation of DM is often affected even before phenotypic changes in CEnCs become apparent. Structural changes in the DM can eventually impair CEnC function, causing cell dysfunction and death. (Petrela & Patel, 2023)

When deriving functional CEnCs from PSCs, it is important to consider ECM production. The differentiated cells must either produce the necessary ECM themselves or be cultured on a substrate that supports cell attachment, differentiation, and maturation. An ideal scenario might involve a substrate that provides sufficient initial support for cell attachment, allowing the cells to begin producing their own ECM as they mature. Next, I will go through substrates possible for culturing both primary and PSC-derived CEnCs.

2.6.1 ECM for culturing CEnCs

An ideal material for culturing CEnCs *in vitro* would be a substrate closely matching the biochemical and biomechanical properties of the *in vivo* tissue (Hazra et al., 2023). The natural ECM for CEnCs is DM to which the cells attach strongly *in vivo*. As previously shortly discussed, the main components of the DM include fibronectin, laminins, collagens, and proteoglycans. (Parekh et al., 2021) Maintenance of the CEn relies also on mechanotransduction pathways mediated by DM and its stiffness regulates the direct relationship between the CEn and DM. The topography of the substrate can modify cell phenotype and this may be related to the spatial and dynamic orientation of integrins that can adapt to the structure of the substrate. (McKay et al., 2020) Next, I will go through some of the components of DM and their potential as *in vitro* substrates as well as the role of integrins.

The most abundant collagens found in DM are types IV and VIII. Type VIII collagen is considered somewhat specific to the DM and is thought to play a role in the transition of nutrients and macromolecules from the aqueous humor into the corneal stroma by forming a hexagonal lattice structure. Collagen type IV is found in aggregates at the interface between the stroma and DM, where it elongates into the CEn layer. This arrangement is believed to facilitate CEnC adhesion. (de Oliveira & Wilson, 2020) As the predominant component of the DM, collagen type IV is an ideal substrate for creating an environment that mimics the native ECM, and it has been successfully used as a coating substrate for culturing human primary CEnCs. Similarly, fibronectin, another component of the DM, has also been successfully utilized as a substrate for primary CEnCs but also for hPSCs as seen from Table 1. (Navaratnam et al., 2015; Song et al., 2021)

Laminins are trimeric glycoproteins built with α -, β -, and γ -chains, with their naming determined by the specific chain composition. For example, chains $\alpha 4$, $\beta 2$, and $\gamma 3$ form laminin-423. Over 15 laminin isoforms have been recognized in different organs, each exhibiting tissue-specific distribution. Laminins are crucial for the development and for the fixing of basement membranes due to trauma. Isoforms such as laminin-511, laminin-521, and laminin-3b11 can self-polymerize to trigger basement membrane regeneration. They also act as a binding site for other ECM components and laminins, facilitating the formation of a fully developed basement membrane. (de Oliveira & Wilson, 2020; Durbeej, 2010) In DM, the laminins present in adults include laminin-511, laminin-521, and

laminin-411, while in infants, laminin-332 is also present (Kabosova et al., 2007; Mas-soudi et al., 2016; Okumura et al., 2015). Among these, laminin-511 and laminin-521 are the predominant laminins at the interface between CEnCs and DM (McKay et al., 2020).

Primary CEnCs express various integrin heterodimers at the interface of DM. The knowledge about these integrins is critical for designing effective substrates for culturing these cells. The key integrin heterodimers expressed in primary CEnCs are $\alpha3\beta1$ and $\alpha6\beta1$, which interact with ligands such as laminin, collagen type IV, nidogen, and fibronectin. These interactions play a pivotal role in regulating CEnC adhesion to DM. Besides promoting the cell adhesion, laminins 411 and 511 help reduce the number of primary CEnCs undergoing EMT. Notably, some integrins expressed by CEnCs also bind ligands beyond those found in DM, including vitronectin and thrombospondin-1, expanding the range of potential substrates for CEnC culture. (McKay et al., 2020)

Matrigel is a widely used commercial cell culture matrix and has also been utilized as a substrate for culturing PSC-derived CEnCs (see Table 1). It is obtained from the Engelbreth-Holm-Swarm mouse sarcoma and mainly contains laminin, collagen IV, and enactin. However, as an animal derived compound, Matrigel has high variability and an increased risk of pathogen transfer, making it less suitable for clinical applications. (E. A. Aisenbrey & Murphy, 2020; Hughes et al., 2010)

2.7 Differentiation efficiency and current problems

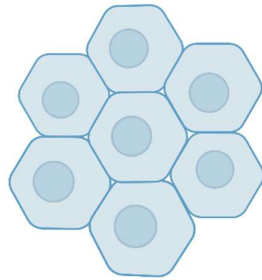
Methods for differentiating CEnC-like cells from hPSCs are still in the early stages of development, with several challenges yet to be addressed. Current protocols are highly complex and some incorporate animal-derived components (see Table 1). For therapeutic applications, it is essential to ensure and characterize that the differentiated cells are both functional and safe. It is also not yet fully known whether the differentiation process affects the DNA of the CEnC-like cells, potentially causing epigenetic or karyotypic changes. One of the most significant challenges, however, is achieving high cell purity. Because of the potential of PSCs, unwanted cell populations may form during differentiation. Because of the low efficiency of the current protocols, the side populations often vary between differentiation batches, emphasizing the need for thorough characterization at every stage of the process. At the end of the differentiation, it is also important that no PSC-associated cells are left in the culture, as these could lead to tumorigenicity. (Català et al., 2022) For example, the protocol developed by Grönroos et al. is fast and effective, but it still has the issue of unwanted cell colonies outcompeting the CEnC-like

cells. These cells resemble mesenchymal-like cells and are unsuitable for the intended purpose. (Grönroos et al., 2021) Despite the protocol's speed, the issue of remaining impurities prevents its use in clinical applications.

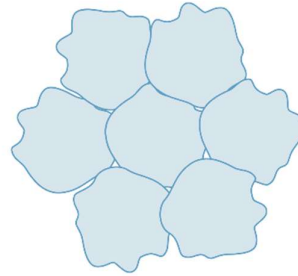
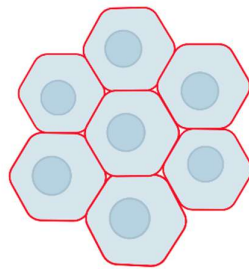
To confirm that the differentiated cells are truly CEnC-like, specific protein markers associated with CEnCs must be used. It is crucial to reliably verify both the genotype and phenotype of these cells when transitioning from the lab to the clinic. As seen from table 1, CEnC-like cells were identified based on CEnC-markers and hexagonal morphology. However, there remains a problem when identifying the CEnCs based on these markers since they are not specific to only CEnCs, as discussed in more detail below.

The most used markers are Na⁺/K⁺ ATPase and ZO-1. However, since these markers are expressed in almost all epithelial cells, and Na⁺/K⁺ ATPase is practically in every cell, the hexagonal morphology is the distinguishing feature that indicates the cells are CEn in nature (Figure 2). In CEnCs, Na⁺/K⁺ ATPase, together with other ion channels, establishes a membrane potential of about -30 mV. It is important in maintaining cell homeostasis. Na⁺/K⁺ ATPase is also hypothesized to have a role in creating a local hyperosmotic gradient to enable fluid flow from the stroma to the anterior chamber. However, the specific mechanism is not known. ZO-1, on the other hand, is a tight junction protein that maintains the leaky barrier properties of CEn and facilitates nutrient movement from the anterior chamber to the cornea through passive diffusion. Both markers exhibit a hexagonal staining pattern, which is not exclusive to the CEn since it is also seen in retinal pigment epithelium (RPE) cells. (Bogerd et al., 2019) Another limitation of these markers is that they are expressed only when cells are confluent and form tight junctions, with their expression decreasing when the cells are no longer in a monolayer (Bartakova et al., 2016). Thus, while these markers are not perfect, they are still useful.

a) Hexagonal apical surface



b) Irregular basal surface

c) Localization of Na⁺/K⁺

d) Localization of ZO-1

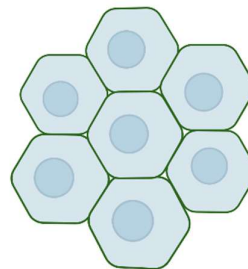


Figure 2. Representation of the hexagonal morphology of the apical surface and localization of the most used markers in the apical surface (red line: Na⁺/K⁺ ATPase, green line: ZO-1). Created with Biorender.com

Other markers utilized for identifying CEnCs are, to name a few, CD166, sodium bicarbonate cotransporter (SLC4A4), aquaporin 1 (AQP1), and N-cadherin (NCAD) (Grönroos et al., 2021). CD166 is an immunoglobulin receptor found in healthy and functional CEnCs and it supports cell-cell adhesion (Smeringaiova et al., 2021). SLC4A4 transporter has an important role in sustaining the solute gradients needed for regulation of water transport from the stroma to the anterior chamber and it is prominently expressed *in vivo* (Frausto et al., 2020). Aquaporins are membrane-spanning proteins that primarily transport water through cell membranes due to differences in osmotic pressure. From the aquaporin family, AQP1 is expressed in CEn, but it is also found in keratocytes and RPE cells, making it a less specific biomarker for CEn. (Verkman et al., 2008) Cadherins are a family of transmembrane glycoproteins that facilitate cell-cell adhesion by binding in a homophilic manner with cadherin molecules on neighboring cells. Among the cadherin family, NCAD is strongly expressed in CEn and is therefore used as a biomarker.

It also reflects the functionality of CEn, as its absence leads to increased CEn permeability. (Vassilev et al., 2012) In addition to the biomarkers indicating differentiated CEnCs, markers specific to NCCs and POM cells can also be used to evaluate the success of differentiation. For example, PITX2 has been used to identify POM cells, while activating enhancer binding protein 2 alpha (AP2 α) is used to identify NCCs (Grönroos et al., 2021). Despite the many options available for identifying CEnC, a unique and specific endothelial marker panel is still lacking. Most of the biomarkers used are also expressed in other cell types, yet they continue to be widely utilized due to the absence of more specific alternatives. (Bogerd et al., 2019)

In conclusion, current differentiation protocols for CEnC-like cells lack the efficiency required to produce pure cell populations suitable for clinical applications. Moreover, the field still lacks a specific marker unique to CEnCs. To advance these cells to clinical use, all these challenges must be addressed to ensure the production of safe and functional cells for patients.

3. AIMS OF THE THESIS

The first aim of this thesis was to enhance the differentiation of hPSCs into CEnC-like cells by addressing challenges such as the formation of unwanted cell colonies. A secondary aim was to shorten the differentiation protocol while maintaining its efficiency. The focus in the first aim was specifically on testing different laminins as culturing substrates and optimizing the concentration of the commonly used substrate, LN521. These tests were based on a previously developed differentiation protocol in the group, with the goal of further optimizing the protocol in terms of both the selection of laminins and time efficiency. Experiments were conducted using one hiPSC line and one hESC line. The outcomes were evaluated by observing cell morphology, analyzing gene expression, and performing immunocytochemistry.

The hypotheses were that combining LN521 with other laminin isoforms would create an environment that more closely mimics DM by incorporating additional ECM components, thereby enhancing differentiation and purity, or that using a completely different laminin isoform alone could improve efficiency. Additionally, I hypothesized that omitting one day from the protocol would not impair the differentiation process.

4. MATERIALS AND METHODS

4.1 hPSC lines

This thesis utilized two previously established hPSC lines: hESC line Regea08/017 and hiPSC line WT001.TAU.bB2 (001b B2 HT). The derivation and culture of hESC line Regea08/017 and hiPSCs line WT001.TAU.bB2 has been previously explained (Grönroos et al., 2021; Skottman, 2010). The research group has supportive statements from the Regional Ethics Committee of the Expert Responsibility area of Tampere University Hospital to derive, culture, and differentiate hESC lines (R05116) and to establish and use hiPSC lines in research (R16116).

This thesis also utilized a patient sample in the form of RNA extracted from human primary CEnCs. The research group has supportive statements from the Regional Ethics Committee of the Expert Responsibility area of Tampere University Hospital to utilize human corneas that are not suitable for transplantation in research (R11134). The RNA was extracted by Outi Melin and provided as a ready sample for positive control in real-time quantitative chain reaction (RT-qPCR) runs. Additionally, the hPSCs batches for the differentiations were kindly provided by laboratory technicians Outi Melin and Hanna Pekkanen. During the writing process of this thesis, results from a new quality control method for hPSCs revealed that the batches of WT001.TAU.bB2 used for matrix and direct induction analyses (excluding the LN332 test) were mixed with the Regea08/017 cell line, creating a pooled sample of both cell lines. This result is based on short tandem repeat (STR) analysis performed by Stemgenomics. This issue has been considered when discussing the results.

4.2 Differentiation of hPSCs to CEnC-like cells

The differentiation into CEnC-like cells was performed following the protocol by Grönroos et al. (2021), with slight modifications. While the control differentiations were done similarly to the original protocol, the matrix tests omitted the one day as undifferentiated hPSC (Figure 3). This so-called direct induction allowed differentiation to begin directly on the desired matrix without prior cell passaging. To assess its functionality, the direct induction approach was also tested using laminin-521 (LN521) as a coating matrix, similarly to the originally established protocol (Grönroos et al., 2021).

Before plating, 12-well plates were coated with either LN521 or the tested matrix (Table 2) and incubated overnight at +4°C. Cells were seeded at densities of 20,000 cells/cm² for control well plates and LN521 concentration tests, and 20,000–50,000 cells/cm² for direct induction and matrix tests. Control cells and cells used in the LN521 concentration tests were cultured as undifferentiated hPSC for one day in Essential 8 Flex medium (E8; Thermo Fisher Scientific, USA). In contrast, cells for the matrix tests were seeded directly into induction medium. The induction medium consisted of KnockOut Dulbecco's Modified Eagle Medium (KO-DMEM), KnockOut serum replacement (KO-SR), Gluta-Max, mercaptoethanol, penicillin/streptomycin, and non-essential amino acids (all from Thermo Fisher Scientific, USA). On day 0, the induction medium was supplemented with 10 µM TGF-β inhibitor SB431542 (SB, StemcellTech, Canada), 4 µM GSK3 inhibitor/WNT pathway activator CHIR99021 (CHIR, StemcellTech), 10 µM retinoic acid (RA, Sigma-Aldrich, United States) and 10 µM Rho kinase inhibitor (ROCKi, StemcellTech). Note that ROCKi was added only for the direct induction cells on day 0 to enhance the attachment of the cells. The RA concentration was gradually reduced over time, halving to 5 µM on day 3 and to 1 µM on day 6, while all other supplements remained constant throughout the culture period. Cell morphology was monitored and imaged during differentiation using a phase contrast light microscope (Nikon Eclipse TE2000-S, Nikon Instruments, Japan).

Table 2. Coatings used in cell cultures.

Coating	Amount	Cell lines
LN521 (controls)	0,987 µg/cm ²	hiPSC (n=6) and hESC (n=4)
LN521 (conc. test)	0,987 µg/cm ²	hESC (n=1)
LN521 (conc. test)	0,75 µg/cm ²	hESC (n=1)
LN521 (conc. test)	0,5 µg/cm ²	hESC (n=1)
LN521 (conc. test)	0,25 µg/cm ²	hESC (n=1)
LN332	0,987 µg/cm ²	hiPSC (n=1) and hESC (n=1)
LN411	0,987 µg/cm ²	hiPSC (n=1) and hESC (n=1)
LN521+LN332	in total 0,987 µg/cm ²	hiPSC (n=1) and hESC (n=1)
LN521+LN411+LN332	in total 0,987 µg/cm ²	hiPSC (n=1)
LN521+LN411	in total 0,987 µg/cm ²	hiPSC (n=1)
LN521 direct induction	0,987 µg/cm ²	hiPSC (n=3) and hESC (n=3)

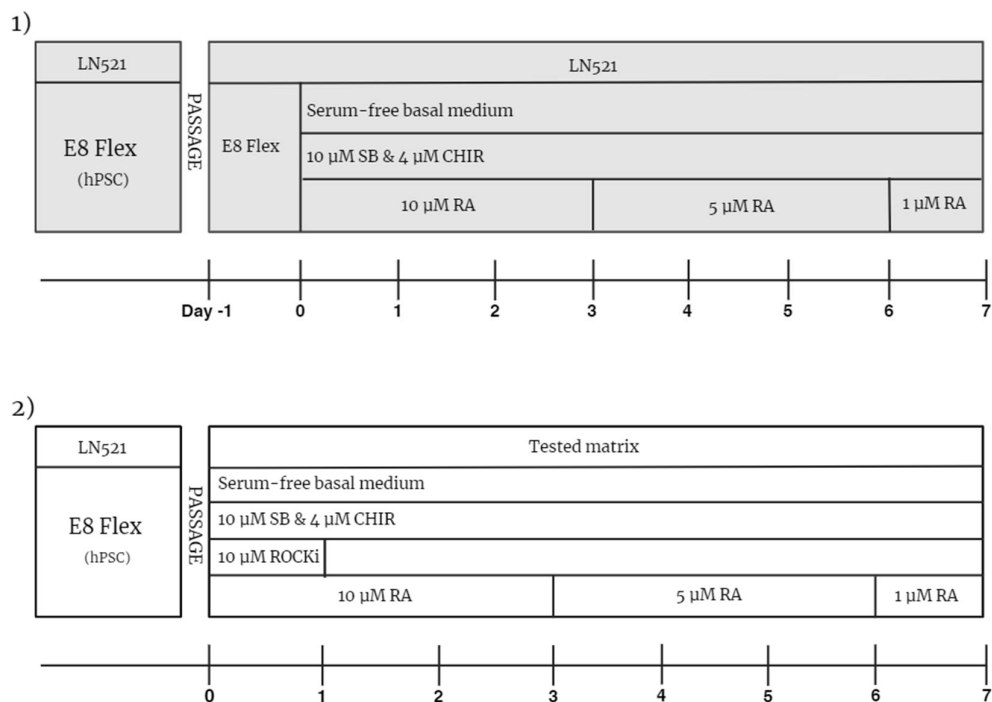


Figure 3. Schematic representation of the differentiation protocol 1) Differentiation protocol according to Grönroos et al. 2021, 2) modified differentiation protocol (direct induction). Abbreviations: LN521= human recombinant laminin 521, E8 Flex = Essential 8 Flex Medium, SB = activin/ BMP/ TGF-beta pathway inhibitor SB431542, CHIR= GSK-3 inhibitor and Wnt pathway activator CHIR99021, ROCKi = Rho kinase inhibitor, and RA = retinoic acid. Created with Biorender.com

4.3 Characterization

4.3.1 Gene expression analysis

Gene expression analysis was performed using RT-qPCR. Total RNA was extracted from undifferentiated hPSCs (day 0) and differentiated cells (day 7) using TRI reagent (Sigma-Aldrich or Invitrogen, USA). Samples were lysed with TRI reagent and chloroform (Sigma-Aldrich) on ice for 15 minutes, followed by centrifugation to separate RNA from cell debris. RNA was then precipitated using isopropanol (Supelco, USA), and the resulting RNA pellet was washed with ethanol (Anora Group, Finland) and resuspended in RNase-free water. RNA concentrations were determined with a NanoDrop-1000 spectrophotometer (NanoDrop Technologies, USA). To remove endogenous DNA, RNA samples were treated with DNase I (Thermo Fisher Scientific, USA) prior to complementary DNA (cDNA) synthesis. Briefly, 1 μ g of RNA per sample was added to an RNase-free tube along with reaction buffer, DNase I, and water. The samples were incubated at 37°C

for 30 minutes, followed by the addition of EDTA and further incubation at 65°C for 10 minutes. For cDNA synthesis, 400–500 ng of RNA per sample was used with the High-Capacity cDNA Reverse Transcription Kit (Applied Biosystems, USA). The obtained cDNA was analyzed with RT-qPCR using TaqMan Gene Expression Assays (Thermo Fisher Scientific, USA) for the following targets: *POU5F1/OCT3/4* (Hs00999632_g1), *PITX2* (Hs04234069_mH), *ATP1A1* (Hs00167556_m1), *TFAP2 α* (Hs01029413_m1), *AQP1* (Hs01028916_m1), and *ALCAM/CD166* (Hs00977641_m1) (Table 3). Each differentiation condition was analyzed using two parallel samples, run in triplicates on the QuantStudio 12K Flex Real-Time PCR System (Applied Biosystems) with 40 cycles, a reaction volume of 15 μ l, and a sample concentration of 2 ng/ μ l. Gene expression was normalized to *GAPDH* (Hs99999905_m1), and relative expression levels were calculated using the $2^{-\Delta\Delta C_t}$ method (Livak & Schmittgen, 2001), with undifferentiated day 0 cells serving as the reference sample. Also, a control without template was included in every run. Statistical analysis was conducted using Mann-Whitney tests in GraphPad Prism software (<https://www.graphpad.com>).

Table 3. Primers used for the gene expression analysis.

Gene	Assay ID
Glyceraldehyde 3-phosphate dehydrogenase (<i>GAPDH</i>)	Hs99999905_m1
POU class 5 homeobox 1 (<i>POU5F1/OCT3/4</i>)	Hs00999632_g1
Paired-like homeodomain transcription factor 2 (<i>PITX2</i>)	Hs04234069_mH
Na ⁺ /K ⁺ ATPase subunit α -1 (<i>ATP1A1</i>)	Hs00167556_m1
Transcription factor AP-2 α (<i>TFAP2α</i>)	Hs01029413_m1
Activated leukocyte cell adhesion molecule (<i>ALCAM/CD166</i>)	Hs00977641_m1
Aquaporin 1 (<i>AQP1</i>)	Hs01028916_m1

4.3.2 Immunocytochemistry

On day 7, cells were fixed with 4% paraformaldehyde (PFA, Sigma-Aldrich) for 15 minutes at room temperature (RT), followed by permeabilization with 0.1% Triton X-100 (Sigma-Aldrich) for 10 minutes at RT. To block nonspecific antibody binding, cells were incubated with 3% bovine serum albumin (BSA, Sigma-Aldrich) for 1 hour at RT.

After blocking, cells were incubated overnight at 4°C with primary antibodies. Controls without the primary antibody were included and incubated only with DPBS (Euroclone, Italy). The expression of OCT3/4, PITX2, CD166, Na⁺/K⁺ ATPase, AP2α and ZO-1 markers was investigated. The following day, the cells were washed three times (5 minutes each) with 1× DPBS (Euroclone). Secondary antibody treatment was performed for 1 hour at RT in the dark with the appropriate 1:800 dilution of secondary antibodies: donkey anti-rabbit IgG (Alexa Fluor 568), donkey anti-mouse IgG (A488), or donkey anti-goat IgG (A488) (all from Molecular Probes, USA), depending on the host of the primary antibody. More detailed information of the used primary and secondary antibodies is listed in supplemental table 1. Nuclei were stained with 1:1000 Hoechst 33342 solution (Invitrogen) at RT for 5 minutes, followed by three washes (5 minutes each) with 1× DPBS. Mounting was performed using either Vectashield Mounting Medium (Vector Laboratories, USA) or ProLong Gold Antifade Mounting Medium (Thermo Fisher Scientific). Stained cultures were stored at 4°C (Vectashield) or RT (ProLong Gold) until further analysis.

Fluorescent imaging was conducted using an Olympus IX51 microscope (Olympus, Japan) with 10× and 20× magnification. Images were processed using ImageJ software (<https://imagej.net/ij/>).

5. RESULTS

The primary aim of this thesis was to evaluate the effects of different laminin isoforms on differentiation efficiency. Specifically, I investigated whether these isoforms reduced the formation of unwanted cell colonies during differentiation while maintaining a polygonal cell morphology. Secondary aim was to determine if a one-day culture period as undifferentiated hPSC prior to induction was necessary for differentiation.

5.1 Matrix tests

Among the laminin isoforms tested, LN411 performed significantly worse than the others (Figure 4). Cells adhered poorly, and only a few colonies formed after one week of culture (see Supplemental Figure 1). Most of the cells floated as clumps in medium. As a result, cell pellets could not be collected, and further testing with this matrix was not conducted. However, the morphology of the remaining colonies was not entirely unfavorable; some cells exhibited a hexagonal morphology, although cell junctions appeared slightly loose, and the cells were bigger than in other conditions. When LN411 was combined with LN521, cell attachment improved, and confluency was achieved, comparable to when LN411 was combined with both LN521 and LN332 simultaneously (Figure 4).

Cells in all other conditions differentiated well, and their morphology was comparable to that of the control cells (Figure 4). By day 7, hexagonal morphology was observed in those parts of the culture where the cells formed a monolayer. In all conditions, cell size got smaller during the differentiation. However, none of the laminin isoforms or their combinations remarkably reduced unwanted cell colonies (indicated by arrows in the Figure 4) or demonstrated superior performance over the control.

The same observations were made with the hESC line 08/017, where only laminins 332 (alone and in a combo with LN521) and 411 were tested. For hESCs, LN411 performed even worse than with hiPSCs, producing cells with fibroblastic-like morphology (Figure 5).

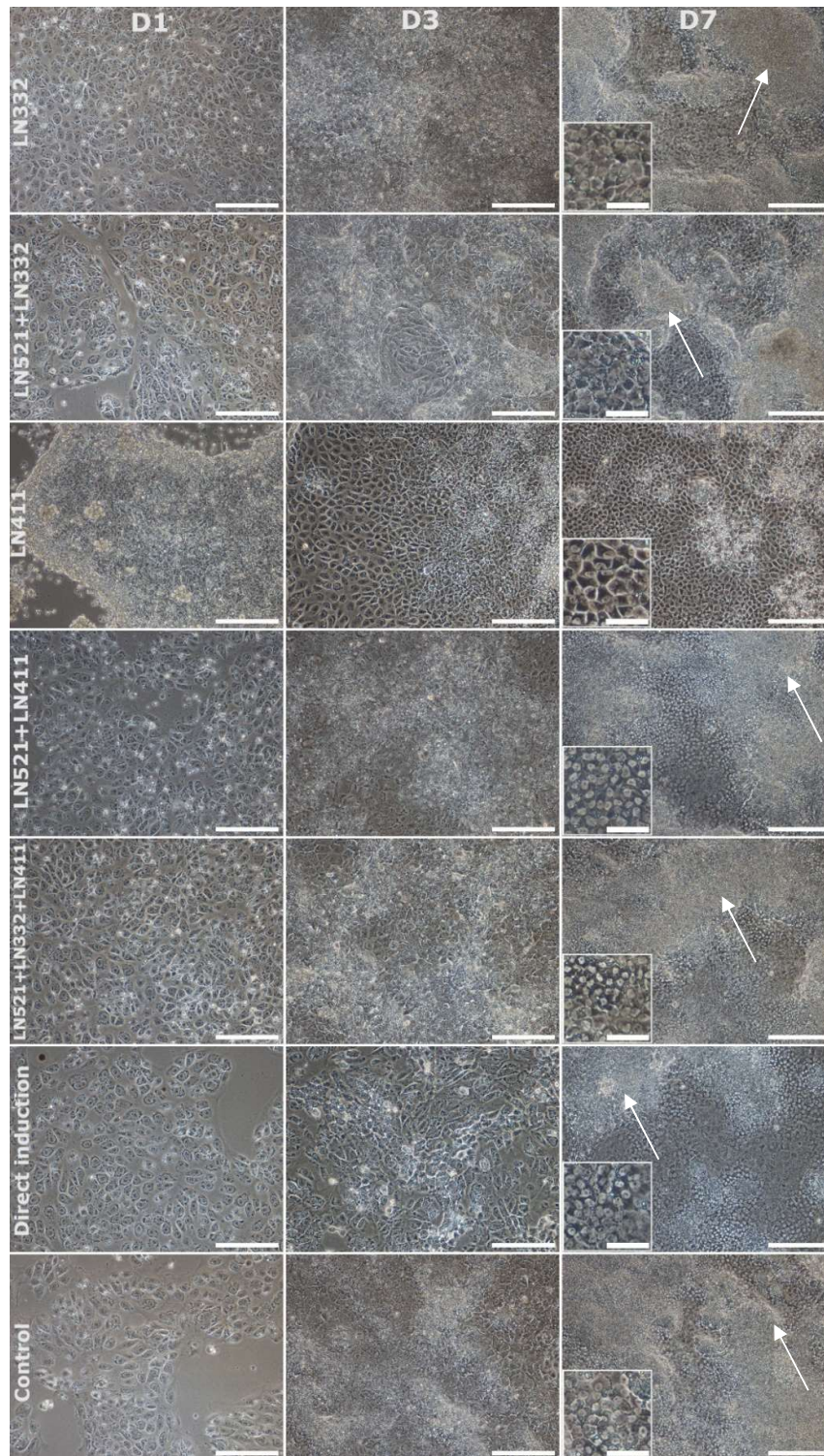


Figure 4. Stereomicroscopy images of the cell morphology with different matrices and culturing conditions during the differentiation towards the CEnC-like cells with 10x magnification and a scale bar of 200 μm (for magnified images 50 μm). Cells differentiated in all conditions but there was still unwanted cell colonies left (white arrows). LN411 was worse than the others (image is not representing the whole culturing well, only the area with cells is shown). Cell line: hiPSC 001b B2 HT. Note: Cell seeding densities varied between conditions.

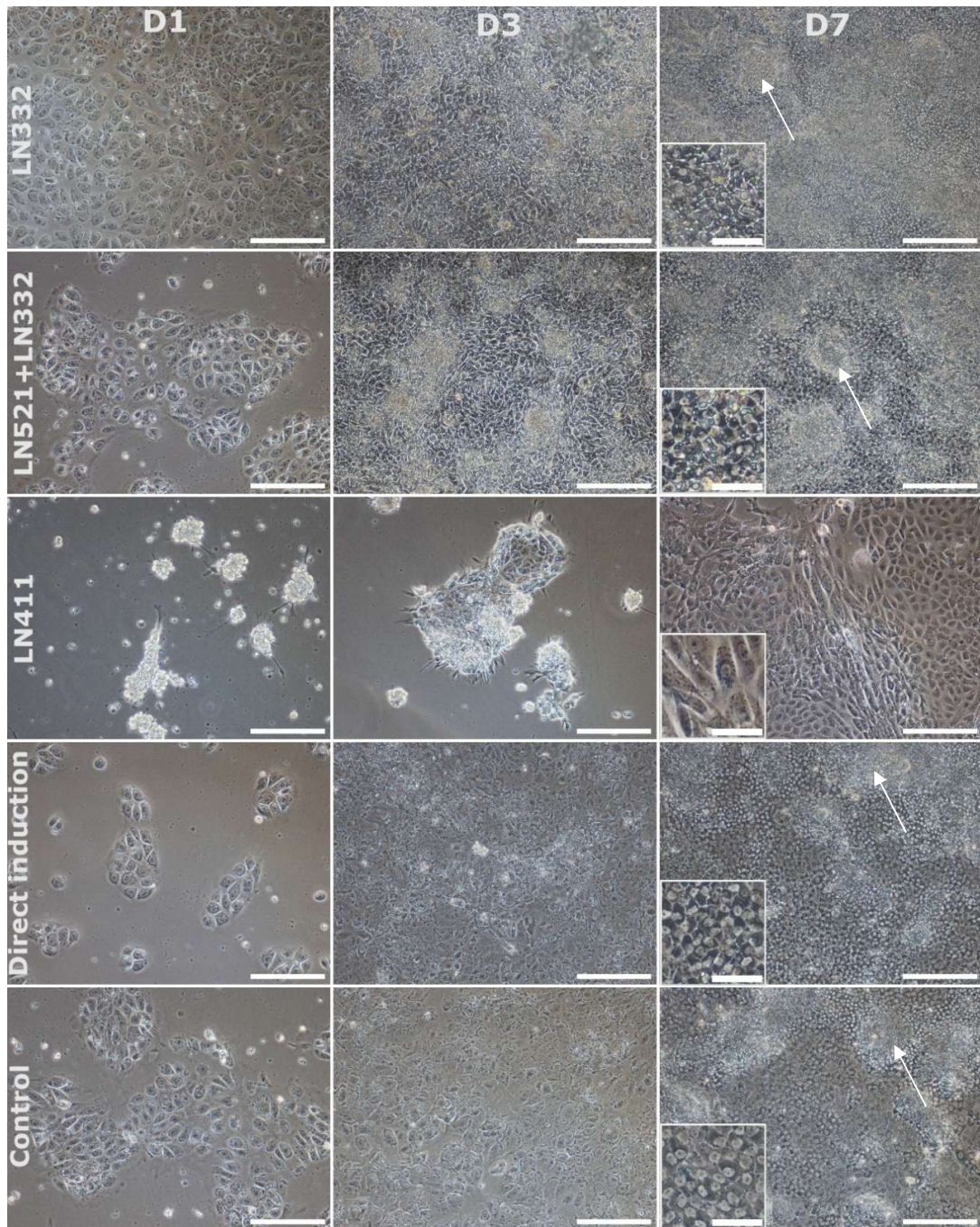


Figure 5. Stereomicroscopy images of the cell morphology with different matrixes and culturing conditions during the differentiation towards the CEnC-like cells with 10x magnification and a scale bar of 200 μm (for magnified images 50 μm). Cells differentiate in all conditions, but on top of LN411 cell do not attach and the morphology is fibroblastic. White arrows indicate unwanted cell colonies. Cell line: hESC 08/017. Note: cell seeding densities varied between conditions.

Gene and protein expression was analysed in all conditions from day 7 differentiated cells. Markers for CEnCs - CD166, Na⁺/K⁺ ATPase, and ZO-1 - as well as POM and NCC markers PITX2 and AP2 α , respectively, were stained. The pluripotency marker OCT3/4 was also tested, but the staining quality was poor, with significant background noise (see Supplemental Figure 2). Therefore, these images were excluded from the panels shown here.

CD166 expression was observed in all conditions, predominantly in cell colonies, making cell morphology less discernible with this marker (Figure 6). Expression was higher in the LN521+LN332+LN411 matrix compared to other conditions, and cell morphology was somewhat visible in the magnified images. The weakest CD166 expression was found in the LN521+LN411 and LN332 matrices. The control condition exhibited the clearest Na⁺/K⁺ ATPase expression, with single cells clearly distinguishable. Other conditions also showed Na⁺/K⁺ ATPase expression, though it was less clear, and dimmer compared to the control (Figure 6). Similar to the expression of CD166, the LN521+LN411 matrix exhibited the weakest expression also in Na⁺/K⁺ ATPase. Interestingly, the protein expression in the LN521+LN332 matrix appeared distinct, with cells resembling "dots" (Figure 6). This condition was mounted with a different mounting medium than the others.

AP2 α , the NCC marker, displayed a similar expression pattern across all conditions, with the LN521+LN411 matrix showing dimmer staining (Figure 7). AP2 α localization was primarily between and around cell colonies, but some positive cells were also found within colonies, particularly in the LN521+LN332 and LN521+LN332+LN411 matrices. The POM marker PITX2 was faintly visible in all conditions except for the control and LN521+LN411 (Figure 7). However, the expression was difficult to distinguish, and the staining intensity was low.

The CEnC marker ZO-1 was observed in all conditions, with magnified images in the LN332, LN521+LN332, and control conditions showing clear cell morphology. In contrast, the LN521+LN411 and LN521+LN332+LN411 matrices exhibited dimmer expression, although still discernible (Figure 8).

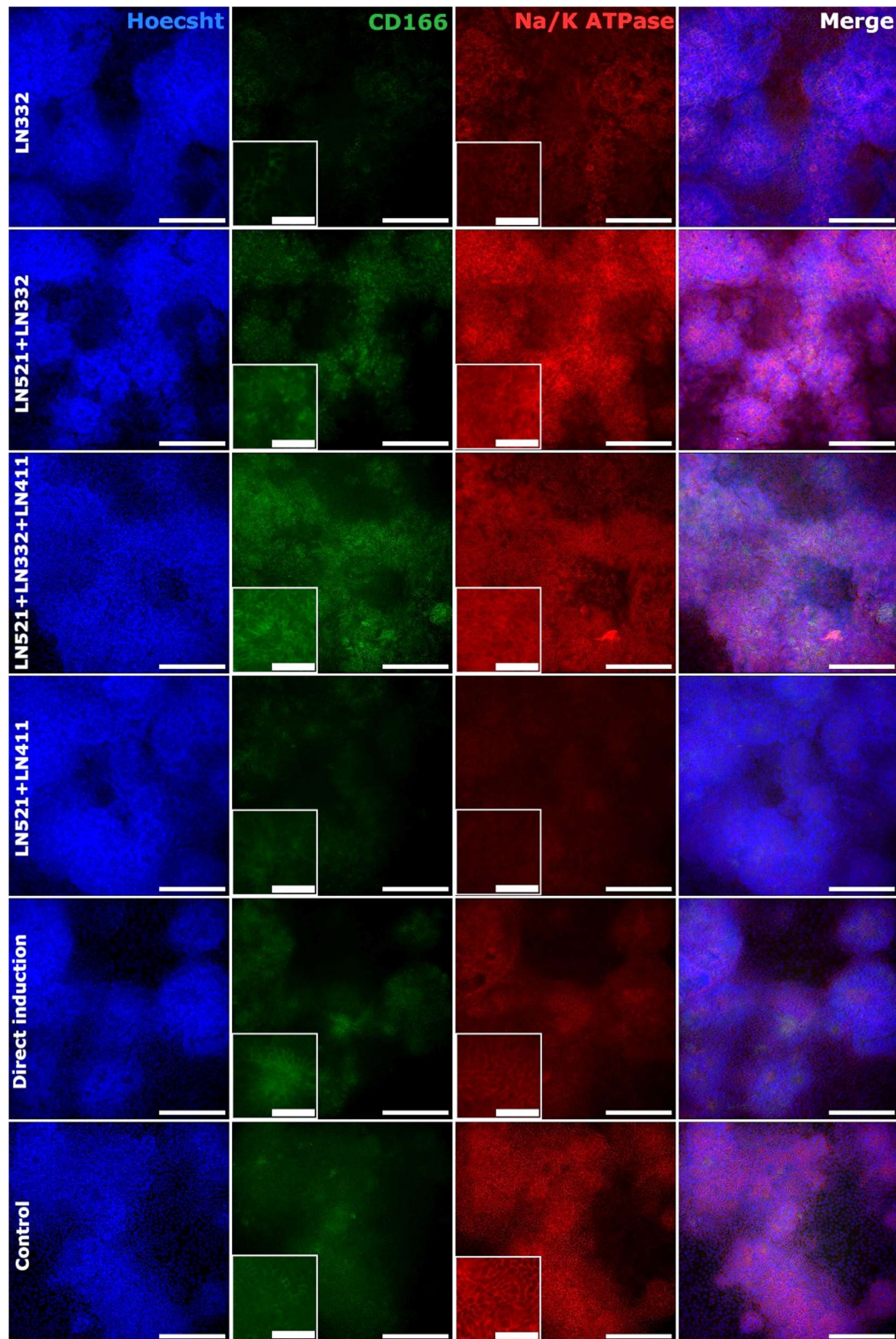


Figure 6. Immunofluorescence images of CEnC markers CD166 (green) and Na⁺/K⁺ ATPase (red) in cells cultured on various matrices and under direct induction compared to control cells. Magnification 20x, scale bar 200 μm (50 μm for magnified images). Cell line: hiPSCs 001b B2 HT.

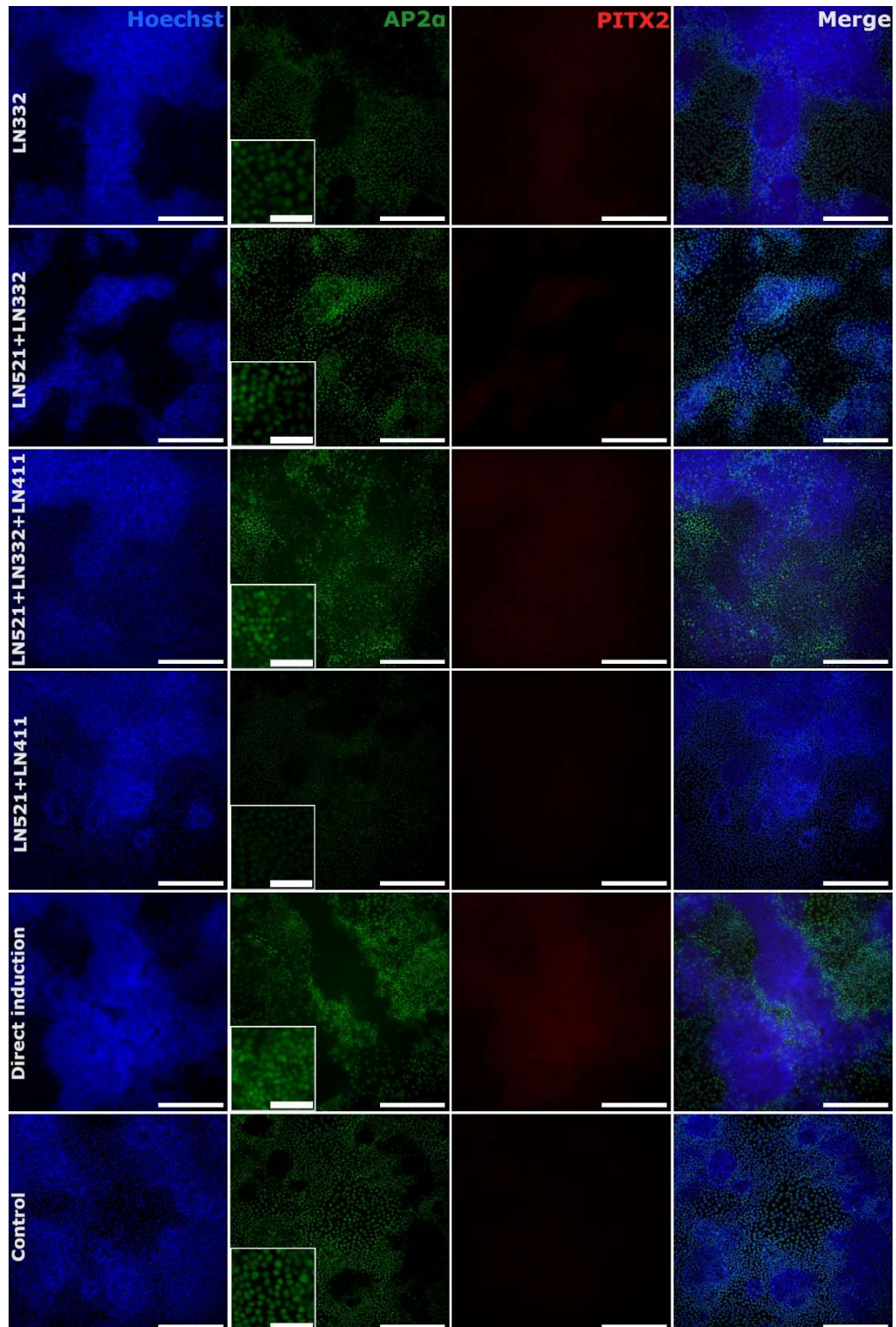


Figure 7. Immunofluorescence images of NCC marker AP2 α (green) and POM-cell marker PITX2 (red) in cells cultured on various matrices and under direct induction compared to control cells. Magnification 20x, scale bar 200 μ m (50 μ m for magnified images). Cell line: hiPSCs 001b B2 HT.

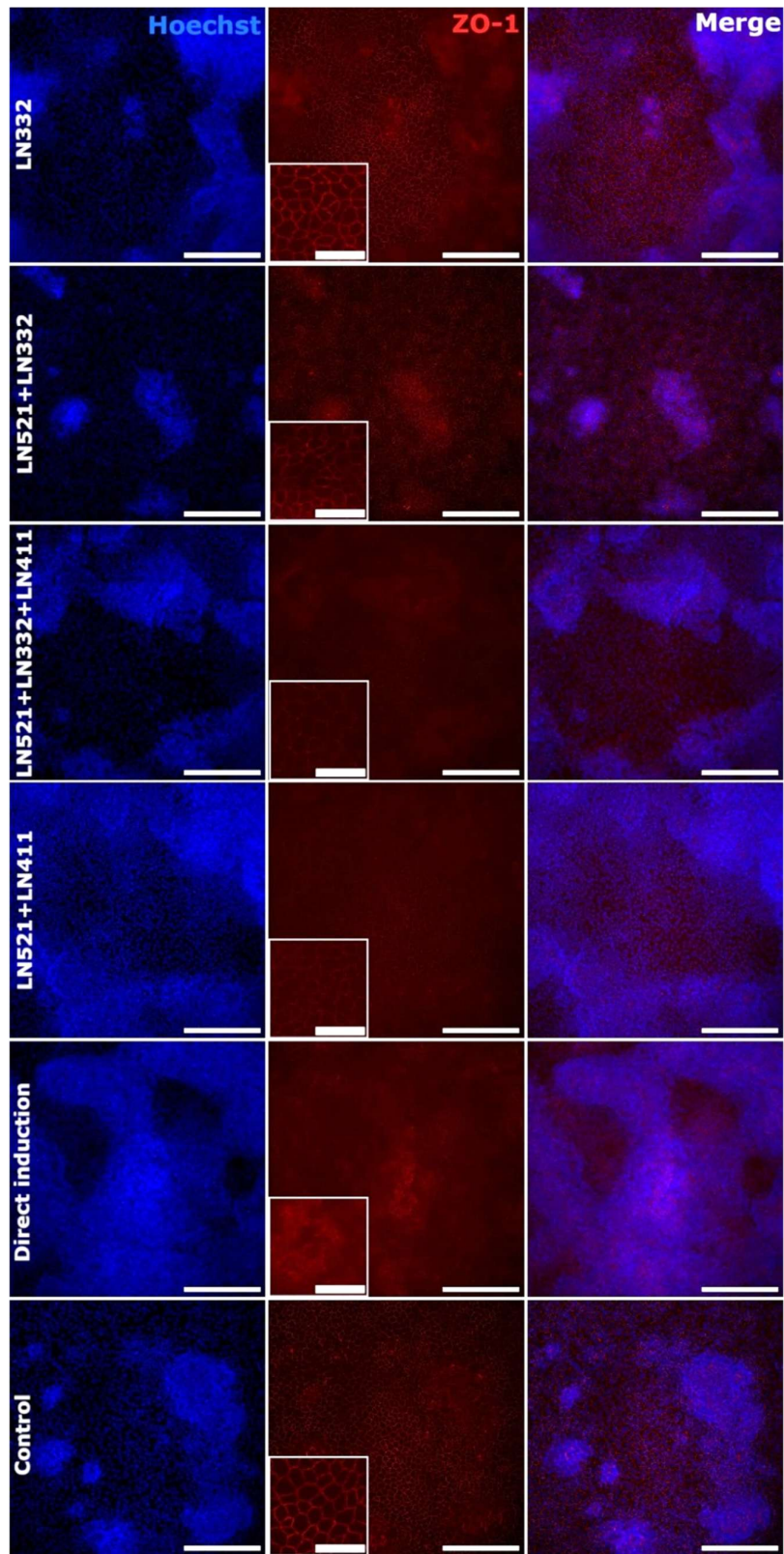


Figure 8. Immunofluorescence images of CEnC marker ZO-1 (red) in cells cultured on various matrices and under direct induction compared to control cells. Magnification 20x, scale bar 200 μm (50 μm for magnified images). Cell line: hiPSCs 001b B2 HT.

The immunocytochemistry results were confirmed with RT-qPCR. None of the matrices brought any advance over the control. The gene expression values stayed around the same magnitude despite the condition (Figure 9). From the tested matrices, LN521+LN411 showed the highest expression levels for nearly all genes, except for *AQP1*, where LN521+LN332+LN411 showed the highest expression (Figure 9f). The control differentiation repeats exhibited notable variability. While some repeats had the highest gene expression levels, others showed very low expression. Overall, the differences between the controls and the matrix tests were not very noticeable. Based on these results, the LN521+LN332 matrix was the least effective, though its poor performance may reflect the unusually low gene expression of its corresponding control, which had the lowest control value across all genes (Figure 9). Since matrix tests were repeated only once, statistical testing was not performed.

With the hESC line, the results from the tested matrices were similar to those obtained with hiPSCs, both in immunofluorescence images and RT-qPCR (Supplemental Figures 3, 4, 5, and 6). Similar to hiPSCs, the hESC control conditions also exhibited considerable variability between repeats (Supplemental figure 6).

hiPSC (001b B2 HT)

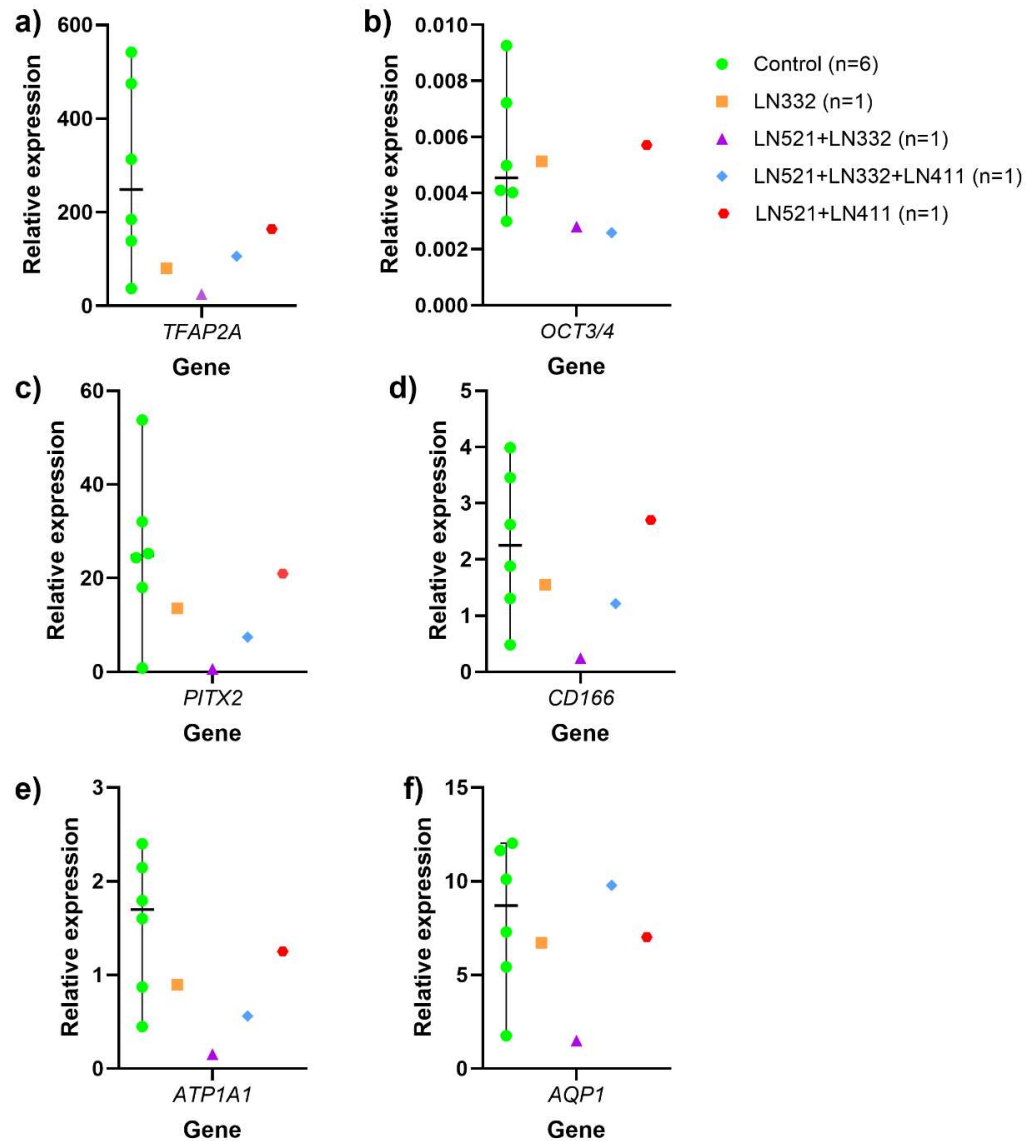


Figure 9. Relative gene expression of day 7 samples analyzed using the $2^{-\Delta\Delta Ct}$ method for a) *TFAP2A*, b) *POU5F1/OCT3/4*, c) *PITX2*, d) *ALCAM/CD166*, e) *ATP1A1*, and f) *AQP1* genes. Cell line: hiPSC 001b B2 HT. Due to high variability among control differentiations, individual repeats are shown as dots on the graph, with their median indicated by a line. Matrix tests were performed once ($n=1$), whereas control differentiation was repeated six times ($n=6$).

5.2 Direct induction

In both cell lines, direct induction on LN521 matrix resulted in cells morphologically similar to the control, but the presence of unwanted cell colonies persisted (Figures 4 and 5). This indicates that the shorter culturing period neither worsen the differentiation or attachment of the cells nor remarkably improve their purity.

Protein expressions were also analysed from the direct induction condition using day 7 differentiated cells and the same markers than with the matrix tests. In hiPSC-derived CEnCs, the CEnC-markers CD166 and Na⁺/K⁺ ATPase showed similar gene expression levels in the direct induction and in the control, although Na⁺/K⁺ ATPase expression was slightly dimmer in direct induction (Figure 6). Cell boundaries were distinguishable in direct induction condition for both markers. The expression of the NCC marker AP2 α was comparable to that in the control and its expression was concentrated around the cell colonies, similar to other conditions. The POM marker PITX2 was expressed more strongly in direct induction compared to the control, where it was practically undetectable (Figure 7). The direct induction condition showed a blurry protein expression of ZO-1, making it challenging to distinguish individual cells. This shows a clear difference from the control, where individual cells were easily distinguishable (Figure 8).

The results of direct induction of hESCs into CEnC-like cells were similar to those observed with hiPSCs (Figure 10). CEnC markers CD166, Na⁺/K⁺ ATPase, and ZO-1 were all expressed in the direct induction condition and were comparable to the control. Cell morphology was clearly visible in the magnified images of both conditions. CD166 and Na⁺/K⁺ ATPase were predominantly localized in cell clumps rather than in the monolayer. Additionally, nuclei (Hoechst) were more easily visualized within the clumps. ZO-1 expression was evenly distributed across the culture, with no localized bright spots observed. The cell borders and morphology were more distinct in the control condition, as there was less background staining. The protein expression of NCC marker AP2 α was clear in both conditions. As with hiPSCs, positive cells were localized around the cell clumps (Figure 10). The POM marker PITX2 was more visible in the direct induction condition than in control. However, its intensity was insufficient to distinguish individual cells (Figure 10). The pluripotency marker OCT3/4 was excluded also from this panel due to high background staining in the wells (see Supplemental Figure 2).

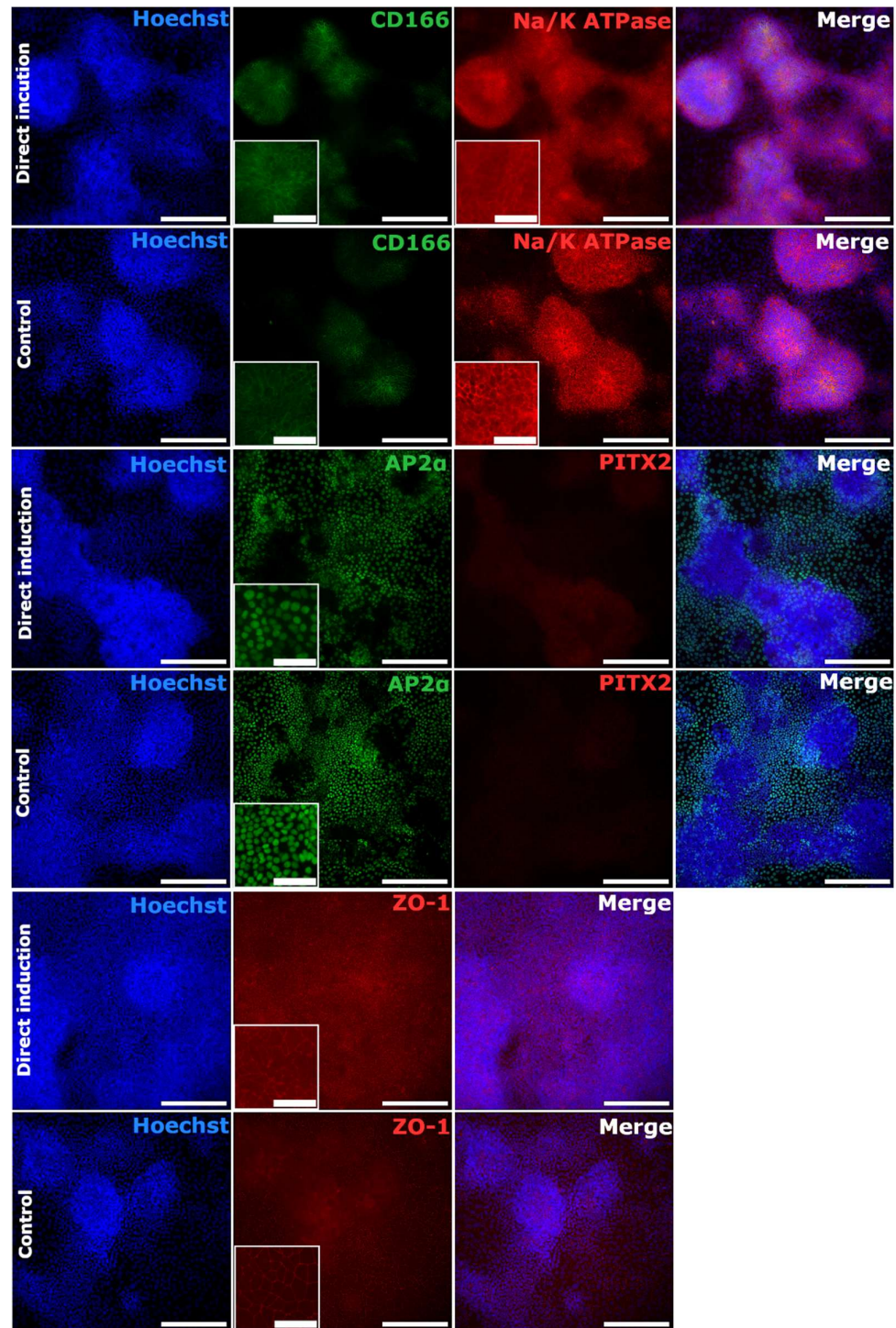


Figure 10. Immunofluorescence images showing stained markers in direct induction compared to controls. Magnification 20x and scale bar 200 μm (50 μm for magnified images). Cell line: hESC 08/017.

The results of direct induction were also analyzed from day 7 cells using RT-qPCR. The differences in gene expression between the direct induction and the control conditions were statistically analyzed using the Mann-Whitney test. None of the genes showed a statistically significant difference between the conditions. Despite the large variation between replicates, the graphs indicate that the differences between conditions were minimal, suggesting that direct induction works similarly to the original protocol (Figure 11). Especially CEnC-markers *ALCAM/CD166*, *ATP1A1*, and *AQP1* were at comparable levels in both conditions, with the control showing slightly elevated expression, as seen in the median values (Figure 11d, e, and f). However, in *ALCAM/CD166*, hiPSC-derived CEnCs had bigger median value for gene expression than its control (Figure 11d). Similarly, POM marker *PITX2* had larger median gene expression in the direct induction condition than in the control (Figure 11c).

Direct induction

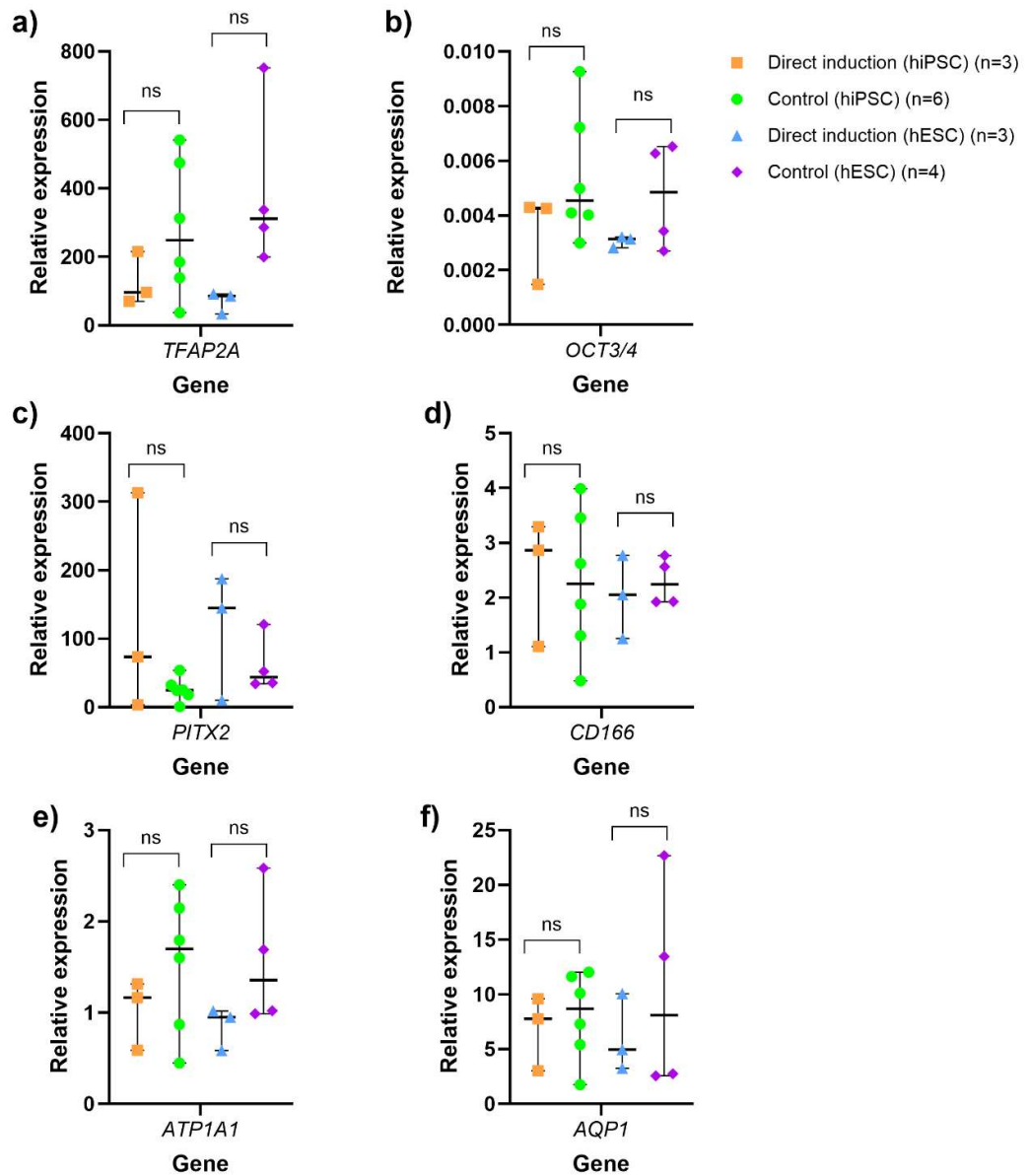


Figure 11. Relative gene expression of day 7 samples analyzed using the $2^{-\Delta\Delta Ct}$ method for a) *TFAP2A*, b) *POU5F1/OCT3/4*, c) *PITX2*, d) *ALCAM/CD166*, e) *ATP1A1*, and f) *AQP1* genes. Cell lines: hESC 08/017 and hiPSC 001b B2 HT. The number of repeats for direct induction in both cell lines was 3 (n=3), while the controls included 6 repeats for hiPSCs (n=6) and 4 for hESCs (n=4).

The control differentiations were also compared to human primary CEnCs, which served as a positive control, to learn how mature our hPSC-derived CEnCs are (Figure 12). Interestingly, *TFAP2A* was remarkably downregulated in primary CEnCs compared to PSC-derived cells (Figure 12a), while *PITX2* showed the opposite trend (Figure 12c). From the CEnC markers, only *ATP1A1* expression levels were comparable between primary cells and PSC-derived cells (Figure 12e). In contrast, the expression of *ALCAM/CD166* (Figure 12d) and *AQP1* (Figure 12f) was higher in primary CEnCs, with a particularly large difference observed in *AQP1*, where the expression levels were thousands of times greater (see Figure 11f for a clearer expression pattern of *AQP1* in hiPSCs and hESCs). Statistical analyses were not performed, as the primary focus was not on the differences between hESC and hiPSC lines.

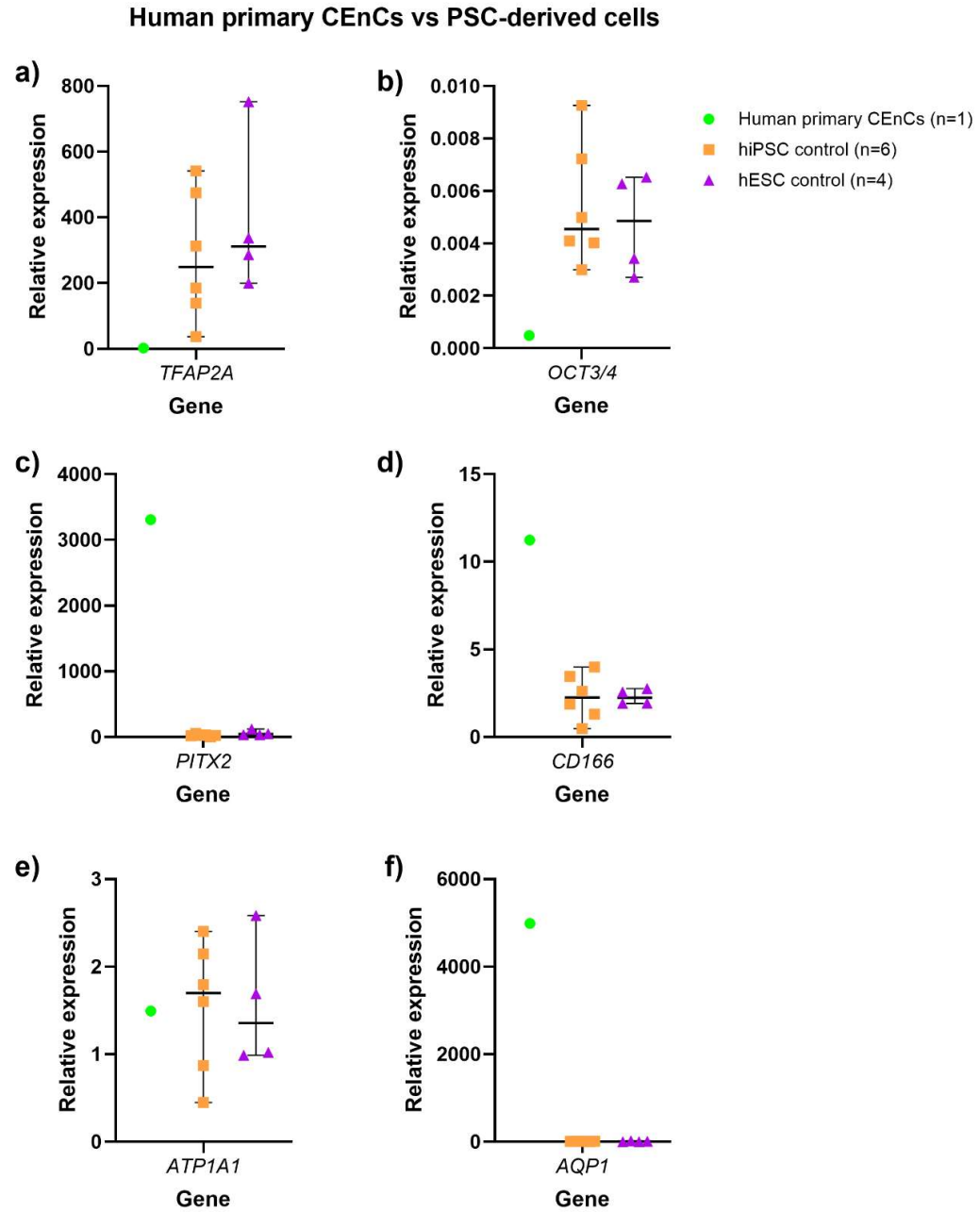


Figure 12. Relative gene expression of day 7 samples and human primary CEnCs analyzed using the $2^{-\Delta\Delta Ct}$ method for a) *TFAP2A*, b) *POU5F1/OCT3/4*, c) *PITX2*, d) *ALCAM/CD166*, e) *ATP1A1*, and f) *AQP1* genes. Cell lines: hESC 08/017 and hiPSC 001b B2 HT.

5.3 LN521 concentration test

As part of the matrix test, different concentrations of LN521 were tested with hESCs. The highest concentration, $0.987 \mu\text{g}/\text{cm}^2$, was selected based on the protocol published by Grönroos et al. (2021), while the manufacturer of LN521, Biolamina, recommends a concentration of $0.51 \mu\text{g}/\text{cm}^2$. It was observed that the concentration of LN521 did not affect cell attachment or the formation of cell clumps (Figure 13). At the lowest concentration ($0.25 \mu\text{g}/\text{cm}^2$), fewer cells were attached on day 1 compared to the other wells. However, by day 7, the outcome was similar to that of the other concentrations, suggesting that LN521 concentrations within the tested range did not have a major impact on the long-term attachment and clump formation of hESCs (Figure 13).

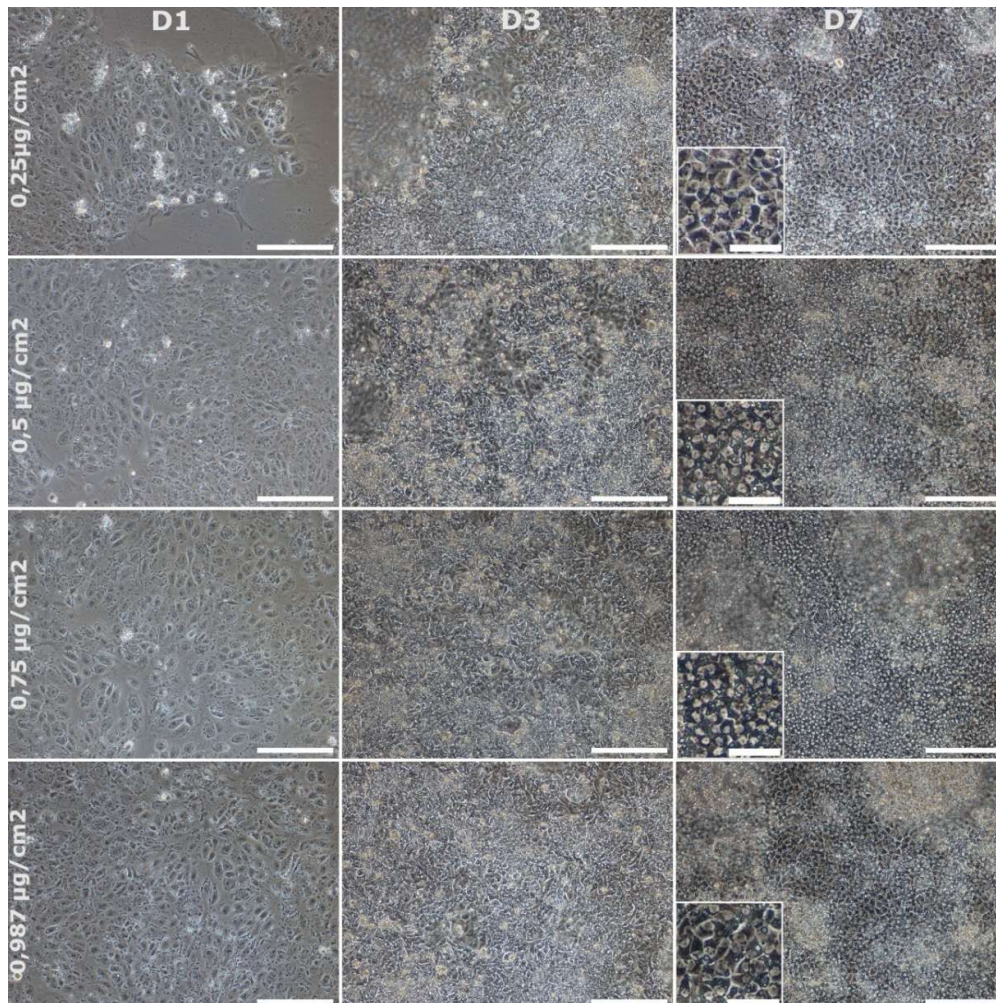


Figure 13. Stereomicroscopy images of cell morphology on top of different concentrations of LN521. Magnification 10x and scale bar $200 \mu\text{m}$ (magnified images $50 \mu\text{m}$). Cell morphology is similar in all concentrations and the cells reach confluency. Cell line: hESC 08/017.

The gene expression analyses were also conducted to the concentration test samples. The differences in gene expression between concentration conditions were analyzed using RT-qPCR (Figure 14). The results indicated that gene expression levels were similar across the different concentrations of LN521. The only notable difference was observed in *AQP1*, where the lower concentrations of LN521 exhibited slightly higher gene expression (Figure 14f). However, this difference was still minimal. Additionally, the gene expression in the distinct 0.987 $\mu\text{g}/\text{cm}^2$ sample showed some variation compared to the control hESC samples, with *CD166* expression being lower (Figure 14d) but comparable to that observed in other LN521 concentration samples. In other genes, the expression level of the distinct 0.987 $\mu\text{g}/\text{cm}^2$ sample was more consistent with the hESC controls.

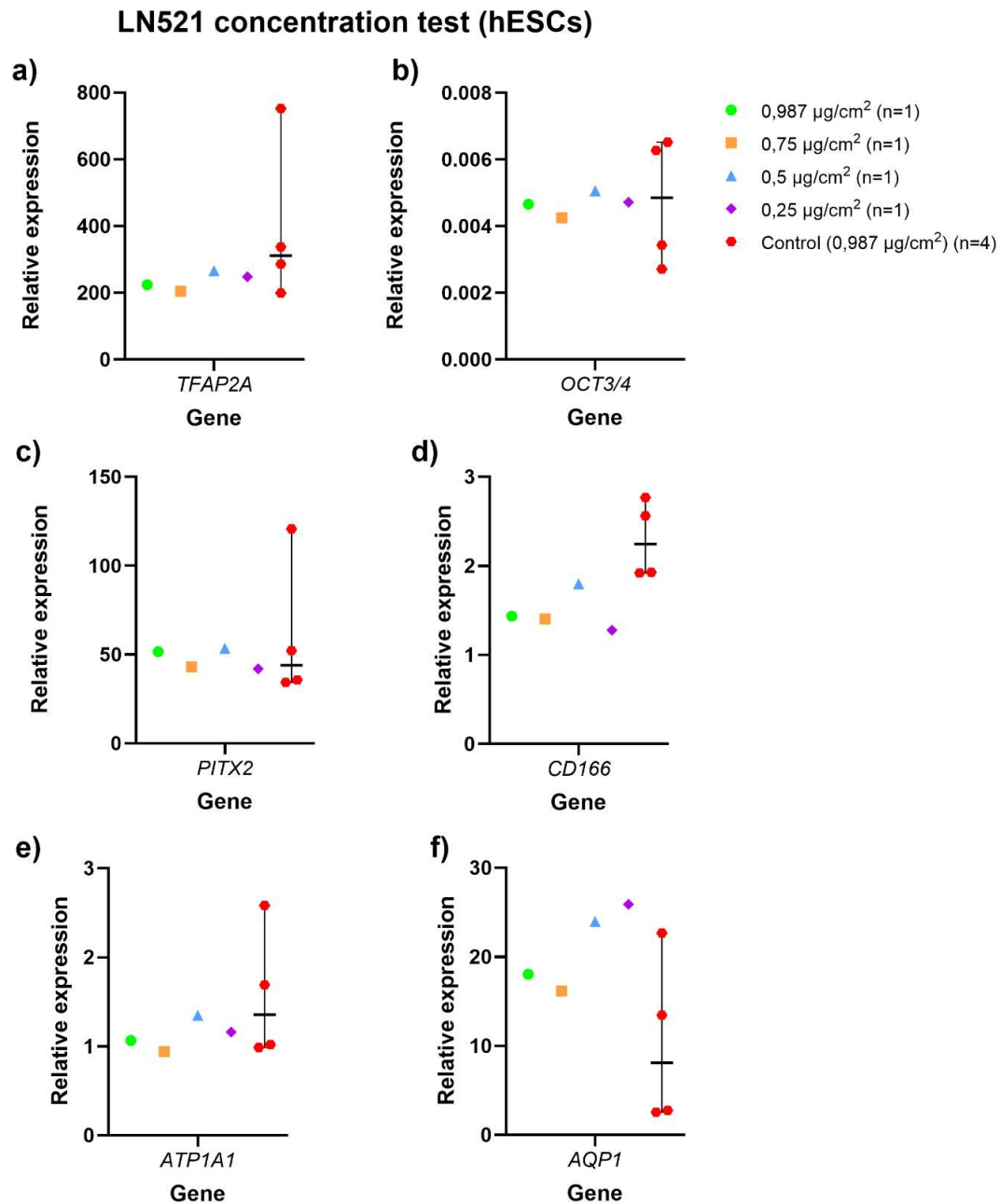


Figure 14. Relative gene expression of day 7 samples analyzed using the $2^{-\Delta\Delta C_t}$ method for a) *TFAP2A*, b) *POU5F1/OCT3/4*, c) *PITX2*, d) *ALCAM/CD166*, e) *ATP1A1*, and f) *AQP1* genes. Cell line: hESC 08/017. The control differentiations for matrix tests of the hESC line (n=4) are combined in the figures, as they were performed with the LN521 concentration of 0.987 $\mu\text{g}/\text{cm}^2$. In the concentration tests, the normal concentration was tested alongside the other concentrations in the same well plate, and therefore, the result is shown independently of the hESC control results.

6. DISCUSSION

The first aim of this thesis was to test different matrices for culturing and differentiating PSCs into CEnC-like cells, as well as to evaluate the effects of varying LN521 concentrations. The second aim was to demonstrate that the differentiation process could be shortened by one day without compromising the protocol's efficiency. This study followed the Grönroos et al. (2021) protocol with slight modifications. The cell lines used were the hiPSC line WT001.TAU.bB2 (001b B2 HT) and the hESC line Regea08/017. The overall goal was to gain insights into factors influencing differentiation efficiency and explore potential improvements to achieve a purer and more homogeneous cell population.

6.1 Matrix tests

As discussed in the literature review, the attachment of CEnCs to DM is partly mediated by integrins expressed on these cells, primarily the heterodimers $\alpha3\beta1$ and $\alpha6\beta1$. The coatings currently in use are based on the known ligands of these integrins, including laminins, collagen type IV, nidogen, thrombospondin-1, and fibronectin (McKay et al., 2020). The commonly used coating substrate in our group, LN521, has been selected based on the knowledge of the major laminins (LN521 and LN511) present in adult DM. Additionally, LN521 is used for hPSC maintenance, which minimizes variability in protocol components. (Grönroos et al., 2021) However, the protocol still requires optimization. This thesis focuses on investigating the effects of different laminin isoforms, as well as combinations of these isoforms, to refine the protocol. The hypothesis was that combining LN521 with other laminin isoforms would create an environment that more closely mimics DM by incorporating additional components of the ECM. It is logical to assume that cells would thrive in an environment that closely resembles the natural ECM.

In this thesis, the difference in gene and protein expression levels between cells seeded on LN521 and those on LN332 was not drastic. While the median gene expression of CEnC markers was higher in control cells, the findings suggest that LN332 also supports PSC-derived cells. In the LN521+LN332 condition, the results were inconsistent between immunofluorescence and qPCR analyses. Immunofluorescence images showed that protein expression in the LN521+LN332 condition was similar to the control. However, qPCR results revealed markedly lower gene expression compared to the median values in the control and values of other matrices. Notably, the control for this cell batch also performed much worse than the other controls, suggesting that the issue lies in the cell

batch rather than being related to the substrate itself. Still, LN332 is not a major component of adult DM, and its presence in keratoconus corneas (Byström et al., 2007) suggests it might not be the optimal choice as a culture substrate in hPSC-CEnCS production. When comparing to the other studies, Yamaguchi et al. investigated the role of LN332 in the adhesion, migration, and proliferation of cultured human primary CEnCs. They found that LN332 significantly improved the attachment of human CEnCs to the dish compared to uncoated dishes. When they compared to fibronectin and collagen type IV-coated dishes, LN332 showed similar attachment efficacy to collagen IV. However, unlike collagen IV, LN332 also promoted cell proliferation, demonstrating its effectiveness for primary cells. Nevertheless, they did not test other laminins, such as LN521, in comparison to LN332. (Yamaguchi et al., 2011)

Interestingly, LN332 is particularly important for RPE cells, which secrete and strongly bind to it via the $\alpha 6\beta 1$ integrin, the same integrin expressed by CEnCs. Despite this shared integrin, RPE cells preferentially bind to LN332 rather than LN521 (S. Aisenbrey et al., 2006). This indicates that laminin preference can be cell-type dependent, even when the same integrins are expressed. The attachment of our hPSC-derived CEnCs for LN332 might suggest that these cells resemble infant CEnCs more than mature adult ones, as reflected also in the qPCR results (Figure 12). However, the fact that Yamaguchi et al. achieved attachment of primary human CEnCs to LN332 suggests that attachment may depend primarily on the integrins expressed. LN332 is a ligand for the $\alpha 3\beta 1$ and $\alpha 6\beta 1$ integrins, both of which are expressed in CEnCs.

In the immunofluorescence images of hiPSCs, LN521+LN411 consistently showed the lowest expression for all markers (Figures 6, 7, and 8). However, in the gene expression analysis, this matrix showed the highest expression levels for nearly all genes, except *AQP1* (Figure 9f), when compared to other matrices tested. This suggests that the low expression observed in immunofluorescence is likely due to a technical issue as the gene expression levels did not show notable variation between conditions. Overall, the LN521+LN411 condition performed decently but did not improve differentiation. Adding LN332 to the combination of LN411 and LN521 did not drastically alter attachment, gene expression levels or protein marker expression. However, PSC-derived CEnCs failed to attach to LN411 alone, forming floating cell clumps.

LN411 is a known component of DM and plays a role in focal adhesions. It appears also to have a role in reducing EMT in human primary CEnCs and serve as a ligand for the primary integrins, $\alpha 3\beta 1$ and $\alpha 6\beta 1$, expressed in these cells. (Ishikawa et al., 2014; McKay

et al., 2020) Toda et al. observed similar results with human primary CEnCs to those presented in this thesis: poor cell attachment to LN411 and pellet formation. In addition, they observed a similar effect with LN332 as with LN411. They found no significant difference between LN521 and LN511 in terms of cell attachment. (Toda et al., 2016) These findings suggest that both primary and PSC-derived CEnCs have a higher affinity for laminin subunit $\alpha 5$ compared to $\alpha 4$ or $\alpha 3$. However, LN411 alone may not be sufficient to maintain cell attachment, potentially requiring interaction with other laminins. This hypothesis is supported by the thesis results, which show that hiPSC-derived CEnCs adhered well when LN411 was combined with LN521 (Figure 4). Furthermore, the gene expression levels in these cells were comparable to the control median (Figure 9).

The effects of different laminins on differentiation were evaluated using immunofluorescence imaging and RT-qPCR. CD166 expression appeared low and was challenging to observe in the immunofluorescence images. It was primarily visible in cell clumps and not in the monolayer regions of the culture (Figure 6). In contrast, Grönroos et al. reported stronger CD166 expression, with single cells clearly visible. This difference may be attributed to their longer culturing time and the fact that some images were taken after passaging, which promotes the formation of a clearer monolayer. Similarly, Na^+/K^+ ATPase was more distinctly illustrated in monolayered cells following passaging (Figure 6). While CD166 and Na^+/K^+ ATPase markers were observed in this experiment, passaging the cells would likely improve marker clarity. The presence of these markers in cell clumps suggests that these cells also exhibit CEnC-like properties, similar to those in the monolayer. However, the lack of a perfect and specific marker for CEnCs prevents definitive identification of cell identity based solely on these markers. Cell morphology provides additional clues about CEnC nature, but it is challenging to assess within cell clumps. Interestingly, AP2 α was more visible outside the cell clumps and remained highly expressed, despite being a NCC marker (Figure 7). This may suggest that our hPSC-derived CEnC-like cells are not fully mature, as they express marker from an earlier developmental stage. In contrast, primary CEnCs exhibit very low *TFAP2A* expression (Figure 12a). However, unlike primary human CEnCs, hPSC-derived cells do not maintain high *PITX2* gene expression (Figure 12c).

Interpreting the immunofluorescence results was challenging at times due to the non-specific staining of the pluripotency marker OCT3/4. Staining was observed in every well, including the secondary control well, but it appeared as vague dots rather than clear nuclear staining (see Supplemental Figure 2). This indicated that the cells did not express OCT3/4, as the staining lacked nuclear localization and was also present in the

secondary control well. Additionally, qPCR data showed very low expression of the *POU5F1/Oct4* gene, which codes for the OCT3/4 protein (Figure 9b). The observed staining could be attributed to autofluorescence or nonspecific binding of the anti-goat antibody to an unintended target. Another challenge was the notable variability between repeats of controls and direct induction experiments. Despite maintaining consistent procedures, gene expression levels varied widely across repeats. This variability suggests that the protocol may require further optimization. Alternatively, it could be due to handling during sample preparation or intrinsic differences between cell batches and passage numbers of the pluripotent stem cells used in differentiation experiments. Notably, gene expression levels are not constant in native tissue, nor even between genetically identical groups of cells (Zheng et al., 2023). Therefore, some degree of variability may persist, even with an optimized protocol. The immunofluorescence images for the LN521+LN332 condition differed from the others, most likely due to the use of a different mounting medium. This well was mounted with ProLong™ Gold Antifade Mounting Medium (Thermo Fisher Scientific), which is designed for use with samples on microscope slides (<https://www.thermofisher.com/order/catalog/product/P10144>). In contrast, all the other wells were mounted with Vectashield Mounting Medium (Vector Laboratories), which is suitable for whole mounts or thicker sections (<https://www.2bscientific.com/suppliers/vector-laboratories/vectashield-antifade-mounting-media>). Since the cell culture was not a monolayer and contained cell clumps, Vectashield may have been more appropriate, leading to better mounting and imaging results.

To assess the reliability of these results, additional repeats would be necessary. However, since each matrix test was accompanied by a control differentiation run simultaneously, it is possible to determine whether a poor outcome was due to the matrix or the cell batch. For example, the poor attachment and survival of cells on LN411 can be attributed to the matrix, as the control differentiation showed normal results. In contrast, surprisingly low gene expression levels observed with LN521+LN332 are more likely due to issues with the cell line, as the control differentiation also produced poor outcomes. Nevertheless, these tests suggest that there is no need to explore further these additional laminins, as the laminins tested here did not show promise in improving the results.

To conclude, while LN332 and LN411 are ligands for $\alpha 3\beta 1$ and $\alpha 6\beta 1$ integrins and LN332 appears to work as a coating, they do not offer advantages over LN521. Additionally, the hypothesis regarding the effect of laminin combinations was not supported. Although cells attached to the laminin combos, they did not improve differentiation or purify the culture. Another challenge is that only LN521 and LN511 are currently available as GMP-

grade products, which are required for transitioning cell production to clinical applications. Therefore, it is not worth spending additional time testing other laminins, as the results did not reveal any significant improvements.

6.2 Direct induction

Reasons for considering the removal of the one-day undifferentiated hPSC step from the protocol were the ability to seed the cells directly on to the desired matrix as well as the intention to shorten the protocol. PSCs are cultured and maintained on LN521, making it challenging to culture them on a different matrix, such as LN332, as it may induce unwanted premature differentiation (Shibata et al., 2018). Since the goal is to apply the differentiation protocol for clinical applications, shortening the timeline by one day would represent a significant resource saving. It would also reduce the need for various components, as the E8 Flex medium could be omitted. The development of cell-based therapies is complex and costly (ten Ham et al., 2021), so strategies to shorten culture time are highly desirable, as time savings also translate into cost savings. In a feasibility study, ten Ham et al. estimated the costs of cell-based therapies and found that the largest portion of the budget is used to facility costs, followed by personnel costs. Both costs could be reduced with a shorter production protocol. Additionally, material costs would decrease, as, for example, the culturing medium would be required for one day less.

The results obtained from immunofluorescence staining and qPCR demonstrated that direct induction works and produces cells similar to those in the control group. The differences in gene expression between the control and direct induction conditions were analyzed using the non-parametric Mann-Whitney test. None of the tests revealed statistically significant differences between the conditions, which was expected due to the large variation and small number of repeats (Figure 11). However, the absence of a drastic difference is a positive outcome, as it suggests that the protocol works without the removed culturing day. The cells seeded straight in induction medium attached well in the presence of ROCK-inhibitor. Nevertheless, it would be useful to test whether the ROCK inhibitor is essential, as omitting it could simplify the protocol when transitioning to clinical use. Additionally, the cell density in the direct induction condition could be optimized further; 20,000 cells/cm² seemed somewhat low, while 50,000 cells/cm² appeared too high.

It is worth noting that all matrix tests were performed using direct induction, which, in a way, increased the number of repeats for this test, despite the use of different matrices.

In these matrix tests, the cells differentiated well, further supporting the effectiveness of the shorter protocol. Overall, based on the results obtained in this thesis, direct induction works well and could be utilized in the future with minor optimization, such as adjusting cell density.

6.3 LN521 concentration test

Based on the cell morphology and qPCR results, the concentration of LN521 does not appear to affect cell fate. Cells attached at all concentrations, and their morphology remained polygonal (Figure 13). The qPCR results also showed that the concentration did not negatively impact differentiation, even when it was three times lower than the commonly used concentration ($0,987 \mu\text{g}/\text{cm}^2$) (Figure 14). According to Biolamina's website, the laminin concentration should be high enough to support cell attachment, proliferation, and growth. Their recommended concentration for a 12-well plate is $0.51 \mu\text{g}/\text{cm}^2$ (<https://biolamina.com/products/laminin-ln-521-stem-cell-matrix/>) and our results indicate that the $0.5 \mu\text{g}/\text{cm}^2$ concentration works well. It might be appropriate to consider the manufacturer's recommendation as the minimum viable concentration. However, Toda et al. found that the binding of human primary CEnCs to LN521 and LN511 is concentration-dependent, with a minimum concentration of 3 ng/ml required for cell attachment (Toda et al., 2016). In contrast, the typical concentration used in our hPSC-derived CEnC cultures is 7501,2 ng/ml, which is much higher than the concentration Toda et al. used. Even with the lowest concentration tested in this thesis ($0.25 \mu\text{g}/\text{cm}^2$), the corresponding amount would be 1900 ng/ml. The strong and specific attachment of integrins expressed on human primary CEnCs to their laminin ligands may explain why such low concentrations are sufficient to enhance attachment. Additionally, primary human CEnCs are fully mature cells, while our cells are undergoing different developmental stages and may not be as mature yet.

To conclude, the concentration of LN521 within the tested range did not appear to affect differentiation or cell attachment. Therefore, lower concentrations can be used when coating the wells, which would help conserve resources. Additionally, the goal is that the hPSC-derived CEnCs could produce their own ECM, as human primary CEnCs do. In this context, the concentration of LN521 would only matter initially, primarily to facilitate cell attachment.

6.4 Study limitations

This thesis has a few study limitations that should be considered. First, a mixed cell line containing both hESCs and hiPSCs was used in almost all experiments involving the hiPSC cell line 001b B2 HT. This may have influenced the results, as generally different hPSCs lines are genetically distinct, because they are obtained from different donors with different genetic background (Rouhani et al., 2014). When two different hPSC lines are mixed, it may impact differentiation potential, resulting in skewed differentiation outcomes and altered gene expression levels. For example, in this thesis the large variation observed in 001b B2 HT control differentiations in the qPCR results might be attributed to the mixed cell line. However, similar variation was also observed in the good quality hESC control differentiations, suggesting that either that line itself contributes to the variability or the overall protocol requires optimization to improve reproducibility. Additionally, the growth phase and other differences of the starting cells may contribute to variability between differentiations. The findings obtained with the mixed hiPSC line do not reliably reflect the true behavior of pure hiPSCs under various matrices or direct induction conditions. Nevertheless, since the results with the mixed hiPSC line were generally similar to those obtained with the pure hESC line, it seems that hiPSCs do not perform worse than hESCs. However, to draw definitive conclusions, further experiments using a pure hiPSC line are necessary.

Another limitation of this thesis is the small sample size and the remarkable variation between experimental repeats, which complicate result interpretation. Additionally, the limited sample size hinders statistical analysis, as both the variation and limited data reduce the reliability of statistical tests. Moreover, only two hPSC lines were used in testing, and not all matrices were tested with the hESC line, which can be considered as a limitation. However, to conserve resources, such screening tests are typically performed with only one repeat. Promising and important results are then selectively repeated, as producing hPSCs and differentiating them is highly expensive.

6.5 Future directions

A lot of optimization remains to be done in the future. Since the other laminin isoforms tested did not provide a better substrate for culturing and differentiating purer CEnC-like cells, alternative options must be explored. Okumura et al. studied human primary CEnC attachment to various laminins and found that blocking integrins $\alpha 3\beta 1$ and $\alpha 6\beta 1$ pre-

vented cell attachment (Okumura et al., 2015). These findings suggest that at least integrins $\alpha3\beta1$ and $\alpha6\beta1$ modulate CEnC attachment by interacting with laminins. Building on this knowledge, substrates targeting integrins expressed on CEnCs could offer promising alternatives to laminins. One such candidate is vitronectin, a glycoprotein located in serum, ECM, and bone, which interacts with integrin $\alpha v\beta3$ to facilitate processes such as cell adhesion and migration (Parekh et al., 2021). This integrin is also expressed in CEnCs (McKay et al., 2020), making vitronectin a potential candidate substrate. Moreover, vitronectin is available as a GMP-grade product, a critical factor for potential clinical applications.

Another aspect worth testing is the medium in which the cells are cultured. Since the unwanted cell colonies did not reduce with changes in the matrix, it is possible that the crucial component lies within the medium. Potential approaches could include changing the entire basal medium or titrating or adjusting the supplements used. Future work should also focus on enhancing the maturation of the differentiated cells, as their gene expression was not at the same level as in human primary CEnCs.

7. CONCLUSIONS

In conclusion, this thesis aims to find ways to improve the differentiation protocol for CEnC-like cells by changing the culturing matrix and modifying the original protocol by Grönroos et al. (2021). This thesis had two main objectives: to investigate the effects of other culturing matrices and different concentrations of the currently used matrix for the differentiation efficiency, and to find out the functionality of the protocol as one day shorter version.

The results did not indicate any better alternatives to the currently used matrix, LN521. The morphology of the cells remained consistent across different matrices, except for LN411, when compared to the control. Similarly, gene and protein expression levels were comparable to the control. Since LN521 is the only tested substrate available as a GMP-compliant product, there is no justification for continuing with the other matrices, even though their performance was not notably worse. The lower concentration of LN521 did not negatively affect differentiation. The findings suggest that lower concentrations are sufficient for cell attachment and differentiation. Leaving one day out of the protocol, or direct induction, was effective and can be used to differentiate CEnC-like cells. However, further optimization of the initial cell seeding density is necessary.

This thesis provides valuable insights into the effects of culture substrates and demonstrates that the protocol can be shortened. Nonetheless, additional optimization is required, as the resulting cell population was neither a purely CEnC-like layer nor fully mature when compared to human primary CEnCs.

REFERENCES

- Aguirre, M., Escobar, M., Forero Amézquita, S., Cubillos, D., Rincón, C., Vanegas, P., Tarazona, M. P., Atuesta Escobar, S., Blanco, J. C., & Celis, L. G. (2023). Application of the Yamanaka Transcription Factors Oct4, Sox2, Klf4, and c-Myc from the Laboratory to the Clinic. *Genes*, *14*(9), Article 9. <https://doi.org/10.3390/genes14091697>
- Aisenbrey, E. A., & Murphy, W. L. (2020). Synthetic alternatives to Matrigel. *Nature Reviews. Materials*, *5*(7), 539–551. <https://doi.org/10.1038/s41578-020-0199-8>
- Aisenbrey, S., Zhang, M., Bacher, D., Yee, J., Brunken, W. J., & Hunter, D. D. (2006). Retinal Pigment Epithelial Cells Synthesize Laminins, Including Laminin 5, and Adhere to Them through $\alpha 3$ - and $\alpha 6$ -Containing Integrins. *Investigative Ophthalmology & Visual Science*, *47*(12), 5537–5544. <https://doi.org/10.1167/iovs.05-1590>
- Ali, M., Khan, S. Y., Gottsch, J. D., Hutchinson, E. K., Khan, A., & Riazuddin, S. A. (2021). Pluripotent stem cell-derived corneal endothelial cells as an alternative to donor corneal endothelium in keratoplasty. *Stem Cell Reports*, *16*(9), 2320–2335. <https://doi.org/10.1016/j.stemcr.2021.07.008>
- Alonso-Alonso, S., Vázquez, N., Chacón, M., Caballero-Sánchez, N., Del Olmo-Aguado, S., Suárez, C., Alfonso-Bartolozzi, B., Fernández-Vega-Cueto, L., Nagy, L., Merayo-Llodes, J., & Meana, A. (2023). An effective method for culturing functional human corneal endothelial cells using a xenogeneic free culture medium. *Scientific Reports*, *13*(1), 19492. <https://doi.org/10.1038/s41598-023-46590-2>
- Bartakova, A., Alvarez-Delfin, K., Weisman, A. D., Salero, E., Raffa, G. A., Merkhofer, R. M., Jr, Kunzevitzky, N. J., & Goldberg, J. L. (2016). Novel Identity and Functional Markers for Human Corneal Endothelial Cells. *Investigative Ophthalmology & Visual Science*, *57*(6), 2749–2762. <https://doi.org/10.1167/iovs.15-18826>

- Bogerd, B. V. den, Zakaria, N., Adam, B., Matthyssen, S., Koppen, C., & Dhubhghaill, S. N. (2019). Corneal Endothelial Cells Over the Past Decade: Are We Missing the Mark(er)? *Translational Vision Science & Technology*, 8(6), 13. <https://doi.org/10.1167/tvst.8.6.13>
- Byström, B., Virtanen, I., Rousselle, P., Miyazaki, K., Lindén, C., & Pedrosa Domellöf, F. (2007). Laminins in normal, keratoconus, bullous keratopathy and scarred human corneas. *Histochemistry and Cell Biology*, 127(6), 657–667. <https://doi.org/10.1007/s00418-007-0288-4>
- Català, P., Thuret, G., Skottman, H., Mehta, J. S., Parekh, M., Ní Dhubhghaill, S., Collin, R. W. J., Nuijts, R. M. M. A., Ferrari, S., LaPointe, V. L. S., & Dickman, M. M. (2022). Approaches for corneal endothelium regenerative medicine. *Progress in Retinal and Eye Research*, 87, 100987. <https://doi.org/10.1016/j.pret-eyeres.2021.100987>
- Chen, J., Ou, Q., Wang, Z., Liu, Y., Hu, S., Liu, Y., Tian, H., Xu, J., Gao, F., Lu, L., Jin, C., Xu, G.-T., & Cui, H.-P. (2021). Small-Molecule Induction Promotes Corneal Endothelial Cell Differentiation From Human iPS Cells. *Frontiers in Bioengineering and Biotechnology*, 9. <https://doi.org/10.3389/fbioe.2021.788987>
- Choi, J. S., Kim, E. Y., Kim, M. J., Khan, F. A., Giegengack, M., D'agostino, R., Criswell, T., Khang, G., & Soker, S. (2014). Factors Affecting Successful Isolation of Human Corneal Endothelial Cells for Clinical Use. *Cell Transplantation*, 23(7), 845–854. <https://doi.org/10.3727/096368913X664559>
- Colman, A., & Dreesen, O. (2009). Pluripotent Stem Cells and Disease Modeling. *Cell Stem Cell*, 5(3), 244–247. <https://doi.org/10.1016/j.stem.2009.08.010>
- de Oliveira, R. C., & Wilson, S. E. (2020). Descemet's membrane development, structure, function and regeneration. *Experimental Eye Research*, 197, 108090. <https://doi.org/10.1016/j.exer.2020.108090>

- DelMonte, D. W., & Kim, T. (2011). Anatomy and physiology of the cornea. *Journal of Cataract & Refractive Surgery*, 37(3), 588. <https://doi.org/10.1016/j.jcrs.2010.12.037>
- Durbeej, M. (2010). Laminins. *Cell and Tissue Research*, 339(1), 259–268. <https://doi.org/10.1007/s00441-009-0838-2>
- Eghrari, A. O., & Gottsch, J. D. (2010). Fuchs' corneal dystrophy. *Expert Review of Ophthalmology*, 5(2), 147. <https://doi.org/10.1586/eop.10.8>
- Espana, E. M., & Birk, D. E. (2020). Composition, structure and function of the corneal stroma. *Experimental Eye Research*, 198, 108137. <https://doi.org/10.1016/j.exer.2020.108137>
- Feizi, S. (2018). Corneal endothelial cell dysfunction: Etiologies and management. *Therapeutic Advances in Ophthalmology*, 10, 2515841418815802. <https://doi.org/10.1177/2515841418815802>
- Frantz, C., Stewart, K. M., & Weaver, V. M. (2010). The extracellular matrix at a glance. *Journal of Cell Science*, 123(24), 4195–4200. <https://doi.org/10.1242/jcs.023820>
- Frausto, R. F., Swamy, V. S., Peh, G. S. L., Boere, P. M., Hanser, E. M., Chung, D. D., George, B. L., Morselli, M., Kao, L., Azimov, R., Wu, J., Pellegrini, M., Kurtz, I., Mehta, J. S., & Aldave, A. J. (2020). Phenotypic and functional characterization of corneal endothelial cells during in vitro expansion. *Scientific Reports*, 10(1), 7402. <https://doi.org/10.1038/s41598-020-64311-x>
- Gain, P., Jullienne, R., He, Z., Aldossary, M., Acquart, S., Cognasse, F., & Thuret, G. (2016). Global Survey of Corneal Transplantation and Eye Banking. *JAMA Ophthalmology*, 134(2), 167–173. <https://doi.org/10.1001/jamaophthalmol.2015.4776>
- Graw, J. (2003). The genetic and molecular basis of congenital eye defects. *Nature Reviews Genetics*, 4(11), 876–888. <https://doi.org/10.1038/nrg1202>
- Grönroos, P., Ilmarinen, T., & Skottman, H. (2021). Directed Differentiation of Human Pluripotent Stem Cells towards Corneal Endothelial-Like Cells under Defined Conditions. *Cells*, 10(2), 331. <https://doi.org/10.3390/cells10020331>

- Gupta, P. K., Berdahl, J. P., Chan, C. C., Rocha, K. M., Yeu, E., Ayres, B., Farid, M., Lee, W. B., Beckman, K. A., Kim, T., Holland, E. J., Mah, F. S., & Committee, from the A. C. C. (2021). The corneal endothelium: Clinical review of endothelial cell health and function. *Journal of Cataract & Refractive Surgery*, 47(9), 1218. <https://doi.org/10.1097/j.jcrs.0000000000000650>
- Hachana, S., & Larrivé, B. (2022). TGF- β Superfamily Signaling in the Eye: Implications for Ocular Pathologies. *Cells*, 11(15), Article 15. <https://doi.org/10.3390/cells11152336>
- Hatou, S., & Shimmura, S. (2019). Review: Corneal endothelial cell derivation methods from ES/iPS cells. *Inflammation and Regeneration*, 39, 19. <https://doi.org/10.1186/s41232-019-0108-y>
- Hazra, S., Dey, S., Mandal, B. B., & Ramachandran, C. (2023). In Vitro Profiling of the Extracellular Matrix and Integrins Expressed by Human Corneal Endothelial Cells Cultured on Silk Fibroin-Based Matrices. *ACS Biomaterials Science & Engineering*, 9(5), 2438–2451. <https://doi.org/10.1021/acsbiomaterials.2c01566>
- He, Z., Forest, F., Gain, P., Rageade, D., Bernard, A., Acquart, S., Peoc'h, M., Defoe, D. M., & Thuret, G. (2016). 3D map of the human corneal endothelial cell. *Scientific Reports*, 6(1), 29047. <https://doi.org/10.1038/srep29047>
- Hirayama, M., Hatou, S., Nomura, M., Hokama, R., Hirayama, O. I., Inagaki, E., Aso, K., Sayano, T., Dohi, H., Hanatani, T., Takasu, N., Okano, H., Negishi, K., & Shimmura, S. (2025). A first-in-human clinical study of an allogenic iPSC-derived corneal endothelial cell substitute transplantation for bullous keratopathy. *Cell Reports Medicine*, 101847. <https://doi.org/10.1016/j.xcrm.2024.101847>
- Hughes, C. S., Postovit, L. M., & Lajoie, G. A. (2010). Matrigel: A complex protein mixture required for optimal growth of cell culture. *PROTEOMICS*, 10(9), 1886–1890. <https://doi.org/10.1002/pmic.200900758>
- Ishikawa, T., Wondimu, Z., Oikawa, Y., Gentilcore, G., Kiessling, R., Egyhazi Brage, S., Hansson, J., & Patarroyo, M. (2014). Laminins 411 and 421 differentially promote

tumor cell migration via $\alpha 6 \beta 1$ integrin and MCAM (CD146). *Matrix Biology: Journal of the International Society for Matrix Biology*, 38. <https://doi.org/10.1016/j.matbio.2014.06.002>

Ittner, L. M., Wurdak, H., Schwerdtfeger, K., Kunz, T., Ille, F., Leveen, P., Hjalt, T. A., Suter, U., Karlsson, S., Hafezi, F., Born, W., & Sommer, L. (2005). Compound developmental eye disorders following inactivation of TGF β signaling in neural-crest stem cells. *Journal of Biology*, 4(3), 11. <https://doi.org/10.1186/jbiol29>

Järveläinen, H., Sainio, A., Koulu, M., Wight, T. N., & Penttinen, R. (2009). Extracellular Matrix Molecules: Potential Targets in Pharmacotherapy. *Pharmacological Reviews*, 61(2), 198–223. <https://doi.org/10.1124/pr.109.001289>

Kabosova, A., Azar, D. T., Bannikov, G. A., Campbell, K. P., Durbeej, M., Ghohestani, R. F., Jones, J. C. R., Kenney, M. C., Koch, M., Ninomiya, Y., Patton, B. L., Paulsson, M., Sado, Y., Sage, E. H., Sasaki, T., Sorokin, L. M., Steiner-Champliaud, M.-F., Sun, T.-T., SundarRaj, N., ... Ljubimov, A. V. (2007). Compositional Differences between Infant and Adult Human Corneal Basement Membranes. *Investigative Ophthalmology & Visual Science*, 48(11), 4989. <https://doi.org/10.1167/iovs.07-0654>

Kels, B. D., Grzybowski, A., & Grant-Kels, J. M. (2015). Human ocular anatomy. *Clinics in Dermatology*, 33(2), 140–146. <https://doi.org/10.1016/j.clinidermatol.2014.10.006>

Kinoshita, S., Koizumi, N., Ueno, M., Okumura, N., Imai, K., Tanaka, H., Yamamoto, Y., Nakamura, T., Inatomi, T., Bush, J., Toda, M., Hagiya, M., Yokota, I., Teramukai, S., Sotozono, C., & Hamuro, J. (2018). Injection of Cultured Cells with a ROCK Inhibitor for Bullous Keratopathy. *New England Journal of Medicine*, 378(11), 995–1003. <https://doi.org/10.1056/NEJMoa1712770>

- Larijani, B., Esfahani, E. N., Amini, P., Nikbin, B., Alimoghaddam, K., Amiri, S., Malekzadeh, R., Yazdi, N. M., Ghodsi, M., Dowlati, Y., Sahraian, M. A., & Ghavamzadeh, A. (2012). Stem Cell Therapy in Treatment of Different Diseases. *Acta Medica Iranica*, 79–96.
- Lewis, P., Silajdžić, E., Brison, D. R., & Kimber, S. J. (2020). Embryonic Stem Cells. In J. M. Gimble, D. Marolt Presen, R. O. C. Oreffo, S. Wolbank, & H. Redl (Eds.), *Cell Engineering and Regeneration* (pp. 315–365). Springer International Publishing. https://doi.org/10.1007/978-3-319-08831-0_19
- Li, Z., Duan, H., Jia, Y., Zhao, C., Li, W., Wang, X., Gong, Y., Dong, C., Ma, B., Dou, S., Zhang, B., Li, D., Cao, Y., Xie, L., Zhou, Q., & Shi, W. (2022). Long-term corneal recovery by simultaneous delivery of hPSC-derived corneal endothelial precursors and nicotinamide. *The Journal of Clinical Investigation*, 132(1). <https://doi.org/10.1172/JCI146658>
- Ljubimov, A. V., & Saghizadeh, M. (2015). Progress in corneal wound healing. *Progress in Retinal and Eye Research*, 49, 17–45. <https://doi.org/10.1016/j.preteyeres.2015.07.002>
- Lwigale, P. Y. (2015). Chapter Four - Corneal Development: Different Cells from a Common Progenitor. In J. F. Hejtmancik & J. M. Nickerson (Eds.), *Progress in Molecular Biology and Translational Science* (Vol. 134, pp. 43–59). Academic Press. <https://doi.org/10.1016/bs.pmbts.2015.04.003>
- Massoudi, D., Malecaze, F., & Galiacy, S. D. (2016). Collagens and proteoglycans of the cornea: Importance in transparency and visual disorders. *Cell and Tissue Research*, 363(2), 337–349. <https://doi.org/10.1007/s00441-015-2233-5>
- McCabe, K. L., Kunzevitzky, N. J., Chiswell, B. P., Xia, X., Goldberg, J. L., & Lanza, R. (2015). Efficient Generation of Human Embryonic Stem Cell-Derived Corneal Endothelial Cells by Directed Differentiation. *PLOS ONE*, 10(12), e0145266. <https://doi.org/10.1371/journal.pone.0145266>

- McKay, T. B., Schlötzer-Schrehardt, U., Pal-Ghosh, S., & Stepp, M. A. (2020). Integrin: Basement membrane adhesion by corneal epithelial and endothelial cells. *Experimental Eye Research*, 198, 108138. <https://doi.org/10.1016/j.exer.2020.108138>
- Meek, K. M., & Knupp, C. (2015). Corneal structure and transparency. *Progress in Retinal and Eye Research*, 49, 1. <https://doi.org/10.1016/j.preteyeres.2015.07.001>
- Menon, S., Shailendra, S., Renda, A., Longaker, M., & Quarto, N. (2016). An Overview of Direct Somatic Reprogramming: The Ins and Outs of iPSCs. *International Journal of Molecular Sciences*, 17(1), Article 1. <https://doi.org/10.3390/ijms17010141>
- Mimura, T., Yamagami, S., & Amano, S. (2013). Corneal endothelial regeneration and tissue engineering. *Progress in Retinal and Eye Research*, 35, 1–17. <https://doi.org/10.1016/j.preteyeres.2013.01.003>
- Moshirfar, M., Odayar, V. S., McCabe, S. E., & Ronquillo, Y. C. (2021). Corneal Donation: Current Guidelines and Future Direction. *Clinical Ophthalmology (Auckland, N.Z.)*, 15, 2963–2973. <https://doi.org/10.2147/OPHTH.S284617>
- Moshirfar, M., Somani, A. N., Vaidyanathan, U., & Patel, B. C. (2024). Fuchs Endothelial Dystrophy. In *StatPearls*. StatPearls Publishing. <http://www.ncbi.nlm.nih.gov/books/NBK545248/>
- Navaratnam, J., Utheim, T. P., Rajasekhar, V. K., & Shahdadfar, A. (2015). Substrates for Expansion of Corneal Endothelial Cells towards Bioengineering of Human Corneal Endothelium. *Journal of Functional Biomaterials*, 6(3), Article 3. <https://doi.org/10.3390/jfb6030917>
- Ng, X. Y., Peh, G. S. L., Yam, G. H.-F., Tay, H. G., & Mehta, J. S. (2023). Corneal Endothelial-like Cells Derived from Induced Pluripotent Stem Cells for Cell Therapy. *International Journal of Molecular Sciences*, 24(15), 12433. <https://doi.org/10.3390/ijms241512433>
- Okumura, N., Kakutani, K., Numata, R., Nakahara, M., Schlötzer-Schrehardt, U., Kruse, F., Kinoshita, S., & Koizumi, N. (2015). Laminin-511 and -521 Enable Efficient In

- Vitro Expansion of Human Corneal Endothelial Cells. *Investigative Ophthalmology & Visual Science*, 56(5), 2933–2942. <https://doi.org/10.1167/iops.14-15163>
- Parekh, M., Ramos, T., O'Sullivan, F., Meleady, P., Ferrari, S., Ponzin, D., & Ahmad, S. (2021). Human corneal endothelial cells from older donors can be cultured and passaged on cell-derived extracellular matrix. *Acta Ophthalmologica (1755375X)*, 99(4), e512–e522. <https://doi.org/10.1111/aos.14614>
- Pera, M. F., Reubinoff, B., & Trounson, A. (2000). Human embryonic stem cells. *Journal of Cell Science*, 113(1), 5–10. <https://doi.org/10.1242/jcs.113.1.5>
- Petrela, R. B., & Patel, S. P. (2023). The soil and the seed: The relationship between Descemet's membrane and the corneal endothelium. *Experimental Eye Research*, 227, 109376. <https://doi.org/10.1016/j.exer.2022.109376>
- Qazi, Y., Wong, G., Monson, B., Stringham, J., & Ambati, B. K. (2010). Corneal transparency: Genesis, maintenance and dysfunction. *Brain Research Bulletin*, 81(2), 198–210. <https://doi.org/10.1016/j.brainresbull.2009.05.019>
- Röck, T., Landenberger, J., Bramkamp, M., Bartz-Schmidt, K. U., & Röck, D. (2017). The Evolution of Corneal Transplantation. *Annals of Transplantation*, 22, 749–754. <https://doi.org/10.12659/AOT.905498>
- Rouhani, F., Kumasaka, N., Brito, M. C. de, Bradley, A., Vallier, L., & Gaffney, D. (2014). Genetic Background Drives Transcriptional Variation in Human Induced Pluripotent Stem Cells. *PLOS Genetics*, 10(6), e1004432. <https://doi.org/10.1371/journal.pgen.1004432>
- Roy, O., Beaulieu Leclerc, V., Bourget, J.-M., Thériault, M., & Proulx, S. (2015). Understanding the Process of Corneal Endothelial Morphological Change In Vitro. *Investigative Ophthalmology & Visual Science*, 56(2), 1228–1237. <https://doi.org/10.1167/iops.14-16166>
- Saghizadeh, M., Kramerov, A. A., Svendsen, C. N., & Ljubimov, A. V. (2017). Concise Review: Stem Cells for Corneal Wound Healing. *Stem Cells*, 35(10), 2105–2114. <https://doi.org/10.1002/stem.2667>

- Shibata, S., Hayashi, R., Okubo, T., Kudo, Y., Katayama, T., Ishikawa, Y., Toga, J., Yagi, E., Honma, Y., Quantock, A. J., Sekiguchi, K., & Nishida, K. (2018). Selective Laminin-Directed Differentiation of Human Induced Pluripotent Stem Cells into Distinct Ocular Lineages. *Cell Reports*, 25(6), 1668-1679.e5. <https://doi.org/10.1016/j.celrep.2018.10.032>
- Singh, V. K., Kalsan, M., Kumar, N., Saini, A., & Chandra, R. (2015). Induced pluripotent stem cells: Applications in regenerative medicine, disease modeling, and drug discovery. *Frontiers in Cell and Developmental Biology*, 3, 2. <https://doi.org/10.3389/fcell.2015.00002>
- Skottman, H. (2010). Derivation and characterization of three new human embryonic stem cell lines in Finland. *In Vitro Cellular & Developmental Biology - Animal*, 46(3), 206–209. <https://doi.org/10.1007/s11626-010-9286-2>
- Smeringaiova, I., Utheim, T. P., & Jirsova, K. (2021). Ex vivo expansion and characterization of human corneal endothelium for transplantation: A review. *Stem Cell Research & Therapy*, 12(1), 554. <https://doi.org/10.1186/s13287-021-02611-3>
- Song, Y., Overmass, M., Fan, J., Hodge, C., Sutton, G., Lovicu, F. J., & You, J. (2021). Application of Collagen I and IV in Bioengineering Transparent Ocular Tissues. *Frontiers in Surgery*, 8. <https://doi.org/10.3389/fsurg.2021.639500>
- Sridhar, M. S. (2018). Anatomy of cornea and ocular surface. *Indian Journal of Ophthalmology*, 66(2), 190–194. https://doi.org/10.4103/ijo.IJO_646_17
- Steinhart, Z., & Angers, S. (2018). Wnt signaling in development and tissue homeostasis. *Development*, 145(11), dev146589. <https://doi.org/10.1242/dev.146589>
- Takahashi, K., Tanabe, K., Ohnuki, M., Narita, M., Ichisaka, T., Tomoda, K., & Yamanaka, S. (2007). Induction of Pluripotent Stem Cells from Adult Human Fibroblasts by Defined Factors. *Cell*, 131(5), 861–872. <https://doi.org/10.1016/j.cell.2007.11.019>
- ten Ham, R. M. T., Nievaart, J. C., Hoekman, J., Cooper, R. S., Frederix, G. W. J., Leufkens, H. G. M., Klungel, O. H., Ovelgönne, H., Hoefnagel, M. H. N., Turner,

- M. L., & Mountford, J. C. (2021). Estimation of manufacturing development costs of cell-based therapies: A feasibility study. *Cytotherapy*, 23(8), 730–739. <https://doi.org/10.1016/j.jcyt.2020.12.014>
- Thomson, J. A., Itskovitz-Eldor, J., Shapiro, S. S., Waknitz, M. A., Swiergiel, J. J., Marshall, V. S., & Jones, J. M. (1998). Embryonic Stem Cell Lines Derived from Human Blastocysts. *Science*, 282(5391), 1145–1147. <https://doi.org/10.1126/science.282.5391.1145>
- Toda, M., Ueno, M., Yamada, J., Hiraga, A., Tanaka, H., Schlötzer-Schrehardt, U., Sotozono, C., Kinoshita, S., & Hamuro, J. (2016). The Different Binding Properties of Cultured Human Corneal Endothelial Cell Subpopulations to Descemet's Membrane Components. *Investigative Ophthalmology & Visual Science*, 57(11), 4599–4605. <https://doi.org/10.1167/iovs.16-20087>
- Trindade, B. L. C., & Eliazar, G. C. (2019). Descemet membrane endothelial keratoplasty (DMEK): An update on safety, efficacy and patient selection. *Clinical Ophthalmology (Auckland, N.Z.)*, 13, 1549–1557. <https://doi.org/10.2147/OPHTH.S178473>
- Van Cruchten, S., Vrolyk, V., Perron Lepage, M.-F., Baudon, M., Voute, H., Schoofs, S., Haruna, J., Benoit-Biancamano, M.-O., Ruot, B., & Allegaert, K. (2017). Pre- and Postnatal Development of the Eye: A Species Comparison. *Birth Defects Research*, 109(19), 1540–1567. <https://doi.org/10.1002/bdr2.1100>
- Van den Bogerd, B., Dhubhghaill, S. N., Koppen, C., Tassignon, M.-J., & Zakaria, N. (2018). A review of the evidence for *in vivo* corneal endothelial regeneration. *Survey of Ophthalmology*, 63(2), 149–165. <https://doi.org/10.1016/j.survophthal.2017.07.004>
- Vassilev, V. S., Mandai, M., Yonemura, S., & Takeichi, M. (2012). Loss of N-Cadherin from the Endothelium Causes Stromal Edema and Epithelial Dysgenesis in the Mouse Cornea. *Investigative Ophthalmology & Visual Science*, 53(11), 7183–7193. <https://doi.org/10.1167/iovs.12-9949>

- Verkman, A. S., Ruiz-Ederra, J., & Levin, M. H. (2008). Functions of aquaporins in the eye. *Progress in Retinal and Eye Research*, 27(4), 420–433. <https://doi.org/10.1016/j.preteyeres.2008.04.001>
- Volarevic, V., Markovic, B. S., Gazdic, M., Volarevic, A., Jovicic, N., Arsenijevic, N., Armstrong, L., Djonov, V., Lako, M., & Stojkovic, M. (2018). Ethical and Safety Issues of Stem Cell-Based Therapy. *International Journal of Medical Sciences*, 15(1), 36–45. <https://doi.org/10.7150/ijms.21666>
- Wagoner, M. D., Bohrer, L. R., Aldrich, B. T., Greiner, M. A., Mullins, R. F., Worthington, K. S., Tucker, B. A., & Wiley, L. A. (2018). Feeder-free differentiation of cells exhibiting characteristics of corneal endothelium from human induced pluripotent stem cells. *Biology Open*, 7(5), bio032102. <https://doi.org/10.1242/bio.032102>
- Williams, A. L., & Bohnsack, B. L. (2019). What's retinoic acid got to do with it? Retinoic acid regulation of the neural crest in craniofacial and ocular development. *Genesis*, 57(7–8), e23308. <https://doi.org/10.1002/dvg.23308>
- Wilson, S. E. (2020). Bowman's layer in the cornea– structure and function and regeneration. *Experimental Eye Research*, 195, 108033. <https://doi.org/10.1016/j.exer.2020.108033>
- Wu, M. Y., & Hill, C. S. (2009). TGF- β Superfamily Signaling in Embryonic Development and Homeostasis. *Developmental Cell*, 16(3), 329–343. <https://doi.org/10.1016/j.devcel.2009.02.012>
- Yamaguchi, M., Ebihara, N., Shima, N., Kimoto, M., Funaki, T., Yokoo, S., Murakami, A., & Yamagami, S. (2011). Adhesion, Migration, and Proliferation of Cultured Human Corneal Endothelial Cells by Laminin-5. *Investigative Ophthalmology & Visual Science*, 52(2), 679–684. <https://doi.org/10.1167/iovs.10-5555>
- Zakrzewski, W., Dobrzyński, M., Szymonowicz, M., & Rybak, Z. (2019). Stem cells: Past, present, and future. *Stem Cell Research & Therapy*, 10(1), 68. <https://doi.org/10.1186/s13287-019-1165-5>

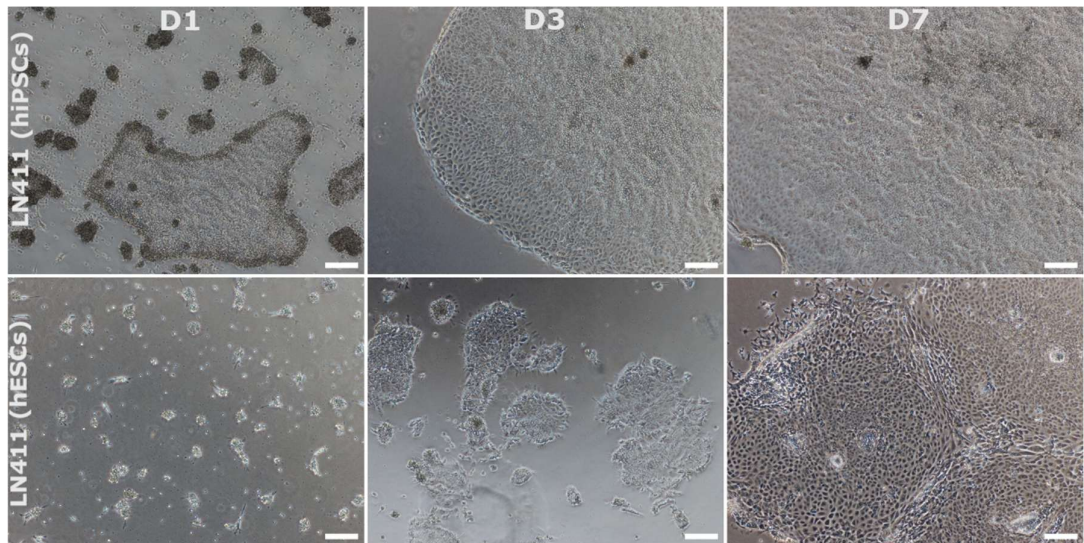
- Zavala, J., López Jaime, G. R., Rodríguez Barrientos, C. A., & Valdez-Garcia, J. (2013). Corneal endothelium: Developmental strategies for regeneration. *Eye*, 27(5), 579–588. <https://doi.org/10.1038/eye.2013.15>
- Zhang, J., McGhee, C. N. J., & Patel, D. V. (2019). The Molecular Basis of Fuchs' Endothelial Corneal Dystrophy. *Molecular Diagnosis & Therapy*, 23(1), 97–112. <https://doi.org/10.1007/s40291-018-0379-z>
- Zhang, K., Pang, K., & Wu, X. (2014). Isolation and Transplantation of Corneal Endothelial Cell-Like Cells Derived from In-Vitro-Differentiated Human Embryonic Stem Cells. *Stem Cells and Development*, 23(12), 1340–1354. <https://doi.org/10.1089/scd.2013.0510>
- Zhao, J. J., & Afshari, N. A. (2016). Generation of Human Corneal Endothelial Cells via In Vitro Ocular Lineage Restriction of Pluripotent Stem Cells. *Investigative Ophthalmology & Visual Science*, 57(15), 6878–6884. <https://doi.org/10.1167/iovs.16-20024>
- Zheng, H., Vijg, J., Fard, A. T., & Mar, J. C. (2023). Measuring cell-to-cell expression variability in single-cell RNA-sequencing data: A comparative analysis and applications to B cell aging. *Genome Biology*, 24(1), 238. <https://doi.org/10.1186/s13059-023-03036-2>

SUPPLEMENTAL METHODS

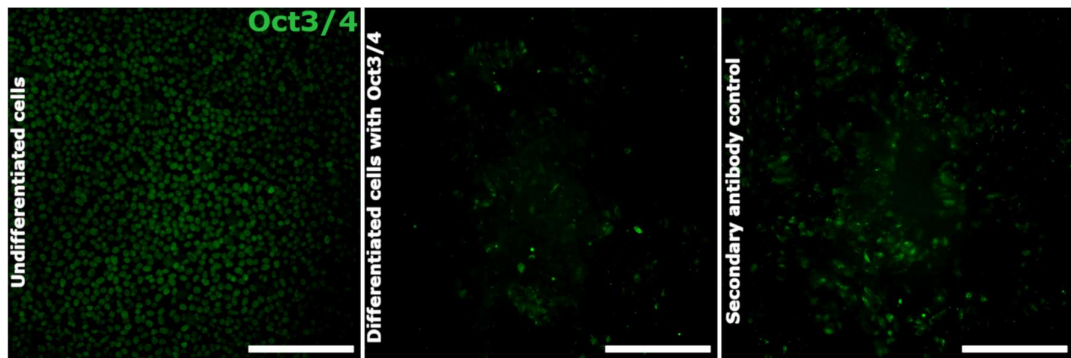
Supplemental table and figures

Supplemental table 1. Antibody information

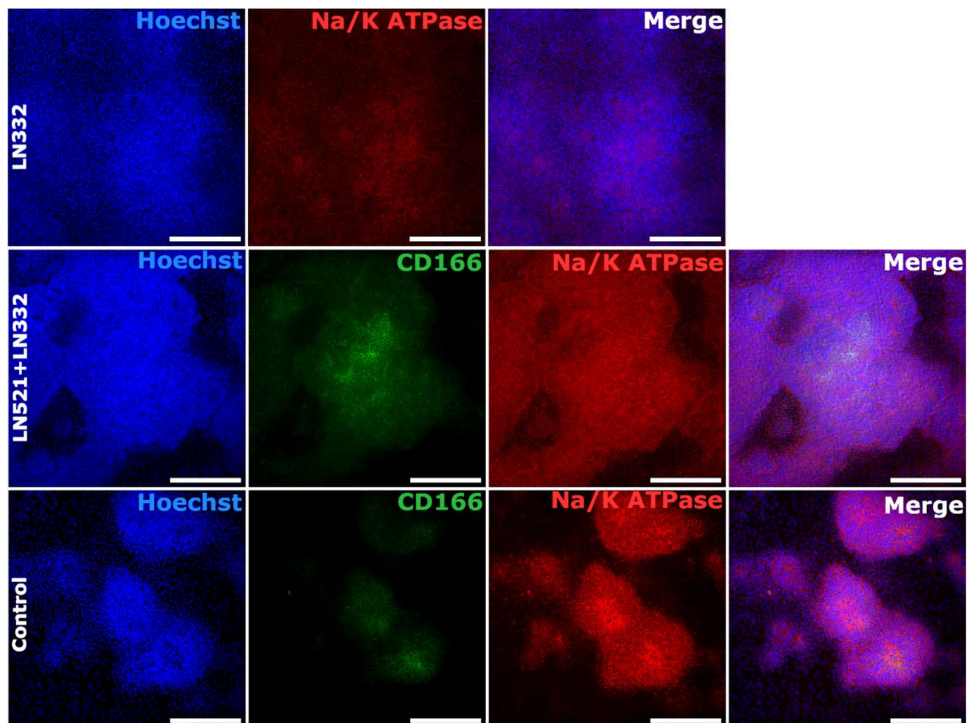
Primary antibodies	Manufacturer	Cat. no.	Dilution	Host	Storage
CD166	BD Pharmigen	559260	1:400	mouse	+4
Na ⁺ /K ⁺ ATPase	Proteintech	55187-1-AP	1:200	rabbit	-20
ZO-1	Invitrogen	61-7300	1:400	rabbit	-20
AP2 α	Santa Cruz	sc-12726	1:400	mouse	+4
PITX2	Thermo Fisher	PA5-11479	1:400	rabbit	-20
Oct3/4	R&D	AF1759	1:400	goat	-20
Secondary antibodies	Manufacturer	Cat. no.	Dilution	Host	Storage
Anti-rabbit A568	Molecular probes	A10042	1:800	donkey	+4
Anti-mouse A488	Molecular probes	A21202	1:800	donkey	+4
Anti-goat A488	Molecular probes	A11055	1:800	donkey	+4



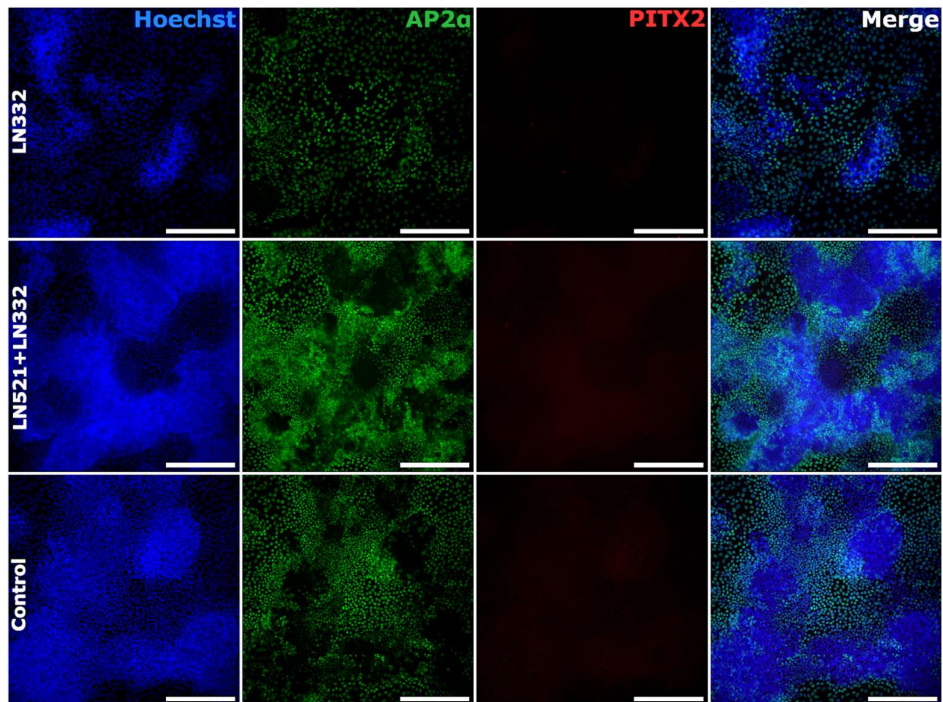
Supplemental Figure 1. Strereomicroscopy images of LN411 coating for hiPSCs and hESCs. Magnification 4x and scale bar 200 μ m. Cells attached poorly on top of LN411.



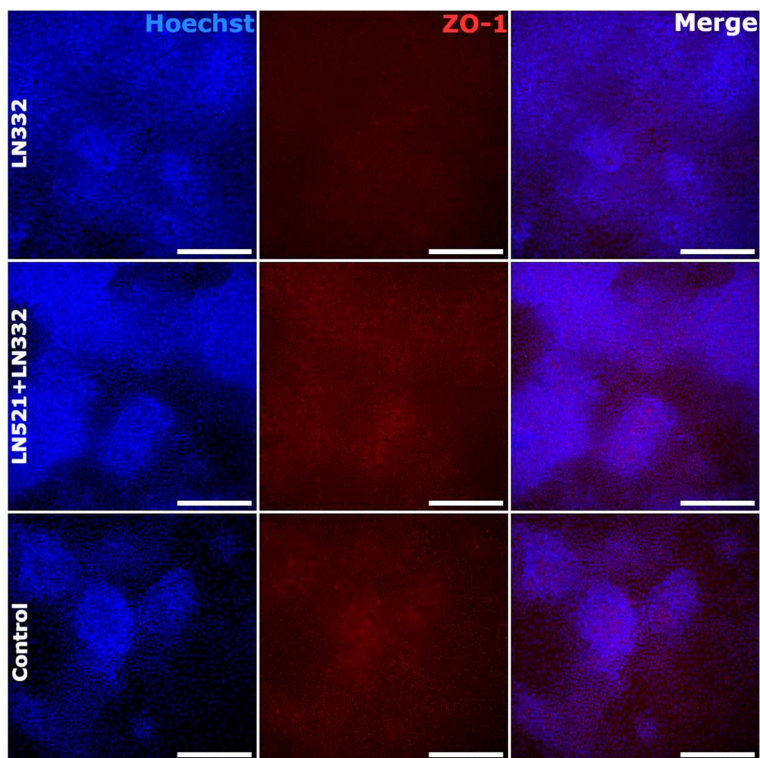
Supplemental Figure 2. Immunofluorescence images of OCT3/4 (green) in undifferentiated cells (left image), differentiated cell stained with OCT3/4 (middle image) and secondary antibody control (right image) where is no OCT3/4 antibody present. Magnification 20x and scale bars 200 μm .



Supplemental Figure 3. Immunofluorescence images of CEnC markers CD166 (green) and Na^+/K^+ ATPase (red) in cells cultured on various matrices compared to control cells. Magnification 20x, scale bar 200 μm . Cell line: hESC 08/017. Note that CD166 staining is missing from condition LN332.

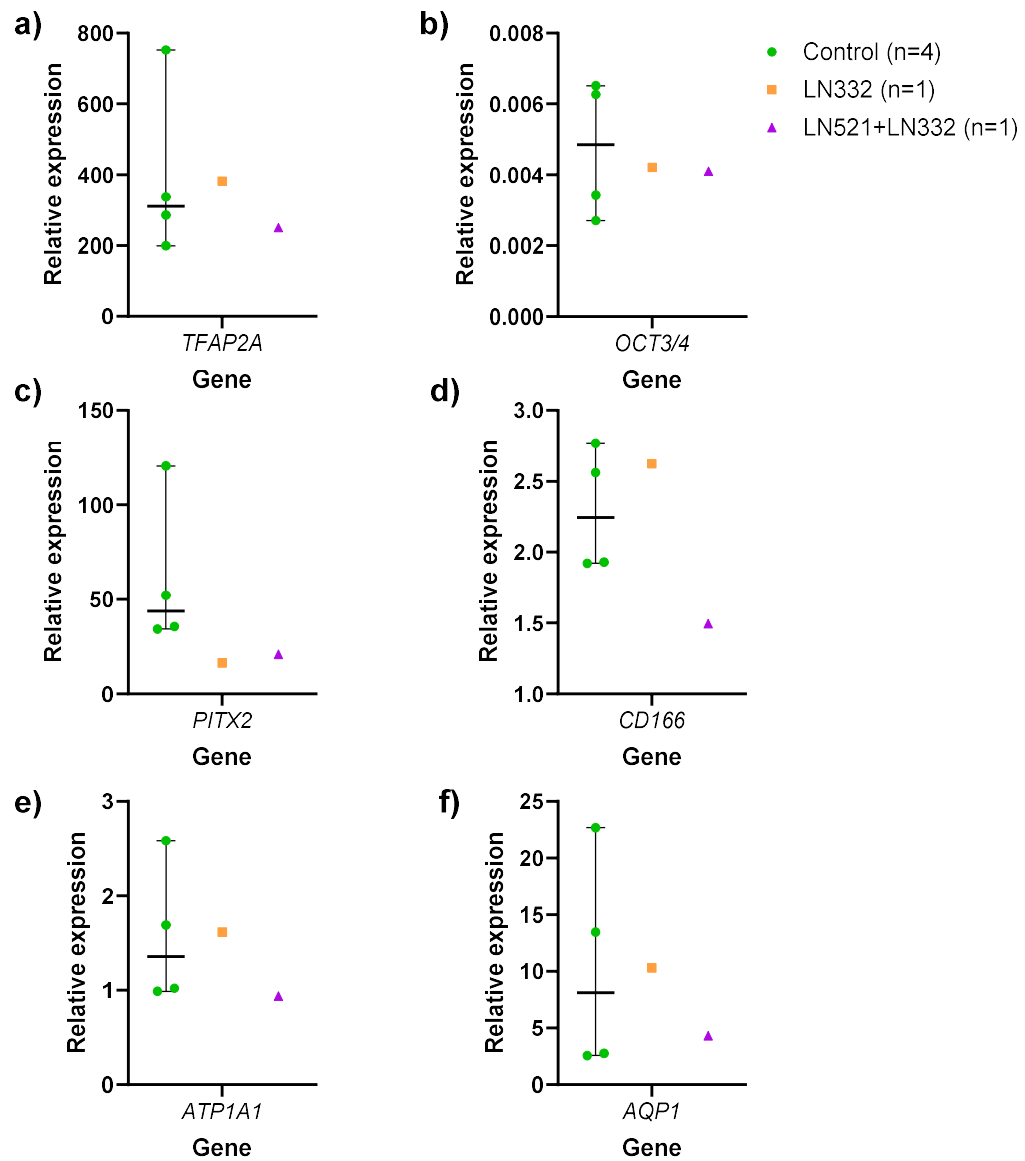


Supplemental Figure 4. Immunofluorescence images of NCC marker AP2 α (green) and POM marker PITX2 (red) in cells cultured on various matrices compared to control cells. Magnification 20x, scale bar 200 μ m. Cell line: hESC 08/017.



Supplemental Figure 5. Immunofluorescence images of CEnC marker ZO-1 (red) in cells cultured on various matrices compared to control cells. Magnification 20x, scale bar 200 μ m. Cell line: hESC 08/017.

hESC (08/017)



Supplemental Figure 6. Relative gene expression of day 7 samples analyzed using the $2^{-\Delta\Delta Ct}$ method for a) TFAP2A, b) POU5F1/OCT3/4, c) PITX2, d) ALCAM/CD166, e) ATP1A1, and f) AQP1 genes. Cell line: hESC 08/017